

Test-Agnostic Long-Tailed Recognition by Test-Time Aggregating Diverse Experts with Self-Supervision

Yifan Zhang¹ Bryan Hooi¹ Lanqing Hong² Jiashi Feng¹

¹National University of Singapore ²Huawei Noah’s Ark Lab

yifan.zhang@u.nus.edu, jshfeng@gmail.com

Abstract

Existing long-tailed recognition methods, aiming to train class-balance models from long-tailed data, generally assume the models would be evaluated on the uniform test class distribution. However, the practical test class distribution often violates such an assumption (e.g., being long-tailed or even inversely long-tailed), which would lead existing methods to fail in real-world applications. In this work, we study a more practical task setting, called **test-agnostic long-tailed recognition**, where the training class distribution is long-tailed while the test class distribution is unknown and can be skewed arbitrarily. In addition to the issue of class imbalance, this task poses another challenge: the class distribution shift between the training and test samples is unidentified. To address this task, we propose a new method, called **Test-time Aggregating Diverse Experts (TADE)**, that presents two solution strategies: (1) a novel skill-diverse expert learning strategy that trains diverse experts to excel at handling different test distributions from a single long-tailed training distribution; (2) a novel test-time expert aggregation strategy that leverages self-supervision to aggregate multiple experts for handling various test distributions. Moreover, we theoretically show that our method has provable ability to simulate unknown test class distributions. Promising results on both vanilla and test-agnostic long-tailed recognition verify the effectiveness of TADE. Code is available at <https://github.com/Vanint/TADE-AgnosticLT>.

1. Introduction

Real-world visual recognition problems typically exhibit a long-tailed training class distribution, where a few classes contain plenty of samples but the others are associated with only a few samples [21, 26]. Due to such imbalance of training sample numbers across classes, training deep network based recognition models becomes challenging: the model can be easily biased towards head (majority) classes and performs poorly on tail (minority) classes [36]. To address this issue, a large number of studies have been conducted to explore the task of long-tailed recognition [8, 18, 24, 44].

Most existing long-tailed recognition methods assume the test class distribution is uniform, *i.e.*, each class has an equal number of test samples. Driven by such an assumption, those methods develop various techniques, *e.g.*, re-sampling [3, 12, 17, 22], re-weighting [2, 8, 10, 19, 29, 34] or ensemble learning [12, 23, 36, 41, 51], to balance the model recognition performance across test classes. However, this assumption does not always hold in real-world applications [16]. Instead, the actual test samples may follow any kind of class distribution, being either uniform, long-tailed as the training data, or even inversely long-tailed to the training data, as shown in Figure 1(a). In such cases, existing methods may perform poorly, especially in the inverse long-tailed one.

To investigate the generalization limitation of existing methods, we evaluate their performance on ImageNet-LT with diverse test class distributions. The results in Table 1 demonstrate the models trained by existing methods suffer from a *simulation bias*, *i.e.*, their prediction strives to simulate a specific preset class distribution. For example, the model trained with the softmax loss simulates the long-tailed training distribution, while the models obtained from existing long-tailed methods try to simulate the uniform test class distribution. More critically, when the test class distribution deviates from the assumed uniform one, the simulation bias still exists and does not adapt, leading the models to generalize poorly.

Motivated by the above observation, we consider a more practical task, namely *test-agnostic long-tailed recognition*, where the training class distribution is long-tailed while the test class distribution is arbitrary and unknown. To address this task, we further explore the simulation property of existing methods (c.f. Table 1) and find that the models learned by different approaches excel at handling test class distributions with different skewness. Motivated by this, we propose to learn multiple skill-diverse experts, from the long-tailed training class distribution, as shown in Figure 1(b). Such a multi-expert model can deal with arbitrary test class distributions as long as these skill-diverse experts can be aggregated adaptively during the test time.

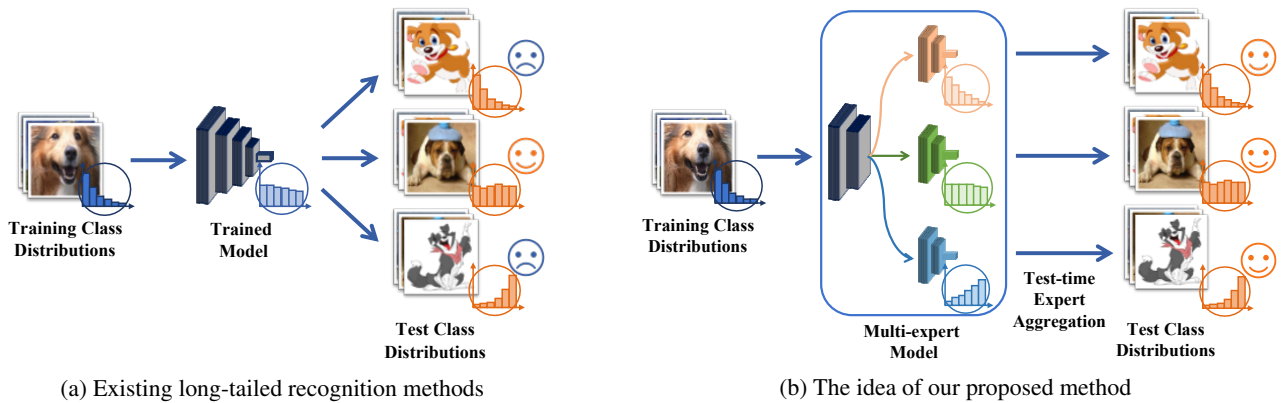


Figure 1. Illustration of the proposed test-agnostic long-tailed recognition. (a) Existing long-tailed recognition methods aim to train models (from long-tailed training data) that perform well on the test data with the uniform class distribution. However, the resulting models cannot deal with real-world test data distribution which can be arbitrary. (b) Our method seeks to learn a multi-expert model, where different experts are skilled in handling different test class distributions. Based on the multi-expert model, our method is able to handle any kind of test class distribution by reasonably aggregating these experts during the test time.

Following the above idea, we propose a novel method, namely Test-time Aggregating Diverse Experts (TADE), with two new solution strategies: skill-diverse expert learning and test-time self-supervised aggregation. Specifically, TADE innovates the expert training scheme by introducing diversity-promoting expertise-guided losses, which train different experts to handle distinct class distributions. In this way, the learned experts would be more diverse than existing multi-expert methods, leading to better ensemble performance, and aggregatedly simulate a wide spectrum of possible class distributions. Then, TADE develops a new self-supervised method, namely prediction stability maximization, to adaptively aggregate these experts for better handling unknown test distribution, using unlabeled test data. We theoretically show that such a test-time learning strategy can simulate arbitrary unknown target class distribution.

TADE achieves new state-of-the-art results on all benchmark datasets, *i.e.*, ImageNet-LT, CIFAR100-LT, Places-LT and iNaturalist 2018. For example, TADE achieves 58.8 top-1 accuracy on ImageNet-LT with 2.5 performance gain than the current state-of-the-art RIDE [36]. More importantly, TADE handles diverse (unknown) test class distributions well, especially the inversely long-tailed class distributions.

We make the following contributions in this work.

- To our best knowledge, we are among the first to study test-agnostic long-tailed recognition, without using any prior knowledge of test class distributions.
- We present two novel methods, *i.e.*, a new skill-diverse expert learning scheme and a novel prediction stability maximization based test-time learning strategy, to solve the challenging task.
- We theoretically show that our test-time self-supervised aggregation strategy can simulate unknown test class distributions, which would be also useful for solving other learning tasks with class distribution shift.

2. Related Work

Long-tailed recognition Most existing long-tailed recognition methods can be categorized into three main classes: class-imbalanced learning, logit adjustment and ensemble learning. Class-imbalanced learning resorts to data resampling [3, 12, 17, 22] or cost-sensitive learning [2, 8, 10, 19, 29, 42, 48, 49] to balance different classes and improve the importance of tail classes. Logit adjustment [16, 26, 31] aims to adjust the output logits of models based on label frequencies during the test time, which encourages a large relative margin between minority and majority classes. Ensemble-based methods [12, 23, 41, 51], *e.g.*, RIDE [36], are based on the multi-expert framework, where each expert seeks to capture heterogeneous knowledge, followed by ensemble aggregation. More discussion on the difference between our method and RIDE can be found in Appendix D.1. As for test-agnostic long-tailed recognition, a very recent study (LADE) [16] assumes the prior of the test class distribution is available and uses the test prior to post-adjust model prediction. In contrast, our method solves this problem without using any test distribution prior.

Test-time training Test-time learning [20, 28] was proposed to handle data distribution shift between training and test data [25, 45, 47]. Recent studies exploit test-time learning to handle dynamic scene deblurring [7] and domain generalization [27, 33]. Inspired by them, we explore this paradigm to address test-agnostic long-tailed recognition.

Self-supervised learning Self-supervised learning [4, 39] is a type of unsupervised learning method. In this field, contrastive learning [14, 21, 35, 40] has been the most popular paradigm. Recently, SimSiam [6] simplifies the contrastive paradigm and only maximizes the similarity between two augmentations of one image. By now, most existing self-supervised learning studies focus on network pre-training [46], but few have explored test-time training.

3. Problem Formulation

Long-tailed recognition aims to learn a classification model from a training dataset with long-tailed class distribution. Let $\mathcal{D}_s = \{x_i, y_i\}_{i=1}^{n_s}$ denote the long-tailed training dataset, where y_i is the class label of the sample x_i . The total number of training samples over C classes is $n_s = \sum_{k=1}^C n_k$, where n_k denotes the sample number of class k . Without loss of generality, we follow a common assumption [16, 22] that the long-tailed classes are sorted by cardinality in decreasing order (i.e., if $i_1 < i_2$, then $n_{i_1} \geq n_{i_2}$), and $n_1 \gg n_C$. The imbalance ratio is defined as $\max(n_k)/\min(n_k) = n_1/n_C$. The test data $\mathcal{D}_t = \{x_j, y_j\}_{j=1}^{n_t}$ is defined in a similar way.

Most existing long-tailed recognition methods assume the test class distribution is uniform (i.e., $p_t(y) = 1/C$), and seek to train models from the long-tailed training distribution $p_s(y)$ that perform well on the uniform test distribution. However, such an assumption does not always hold in practice. The actual test class distribution in real-world applications may also be long-tailed (i.e., $p_t(y) = p_s(y)$), or even inversely long-tailed to the training data (i.e., $p_t(y) = \text{inv}(p_s(y))$). Here, $\text{inv}(\cdot)$ denotes that the long-tailed order of classes is flipped. As a result, the models learned by existing methods may fail when the actual test class distribution is different from the assumed one.

To address this, we seek to solve a more practical long-tailed recognition problem, i.e., **Test-agnostic Long-tailed Recognition**. This task aims to learn a recognition model from long-tailed training data, where the resulting model will be evaluated on multiple test sets that follow different (unknown) class distributions $p_t(y)$. This task is difficult due to the integration of two challenges: (1) severe class imbalance in the training data makes model learning difficult; (2) unknown class distribution shift between training and test data (i.e., $p_t(y) \neq p_s(y)$) makes the model hard to generalize. To address this task, we propose a novel method, namely Test-time Aggregating Diverse Experts.

4. Method

4.1. Motivation and Method Overview

We first analyze why existing long-tailed recognition methods cannot handle test-agnostic long-tailed recognition, followed by elaborating on the motivation and details of our proposed method.

Observation We evaluate some representative long-tailed learning methods [16, 19, 22, 36, 50] on diverse test class distributions, including the uniform, forward long-tailed and backward long-tailed ones. The results are given in Table 1. The “Forward- N ” and “Backward- N ” indicate the cases where test samples follow the same long-tailed distribution as training data and inversely long-tailed to the training data, with the imbalance ratio N , respectively.

Table 1. Top-1 accuracy of existing methods on ImageNet-LT with different test class distributions, including uniform, forward and backward long-tailed ones with imbalance ratios 5, 25 and 50, respectively. The results show that each method performs very similarly in different test class distributions in terms of their performance of many-shot, medium-shot and few-shot classes.

Test Dist.	Softmax			Decouple-LWS [22]			Balanced Softmax [19]		
	Many	Med.	Few	Many	Med.	Few	Many	Med.	Few
Forward-50	67.5	41.7	14.0	61.2	49.5	27.9	63.5	47.8	37.5
Forward-25	67.6	41.7	14.1	61.8	47.4	30.4	64.0	48.2	33.5
Forward-5	67.6	40.9	13.9	60.9	49.0	30.3	63.8	47.5	32.3
Uniform	68.1	41.5	14.0	61.8	47.6	30.9	64.1	48.2	33.4
Backward-5	67.5	41.9	14.0	61.9	48.0	30.8	64.1	48.5	33.5
Backward-25	68.0	42.0	14.4	61.3	48.8	31.1	63.7	48.7	33.2
Backward-50	70.9	41.1	13.8	66.2	44.9	30.9	66.5	48.4	33.2

Test Dist.	MiSLAS [50]			LADE w/o prior [16]			RIDE [36]		
	Many	Med.	Few	Many	Med.	Few	Many	Med.	Few
Forward-50	61.6	50.0	33.3	63.5	46.4	33.1	68.3	51.6	36.8
Forward-25	61.6	50.1	36.9	64.0	47.6	35.9	68.1	51.2	38.5
Forward-5	61.9	49.1	32.0	64.0	47.0	33.8	68.3	52.4	35.9
Uniform	62.0	49.1	32.8	64.4	47.7	34.3	68.0	52.9	35.1
Backward-5	62.2	49.1	32.7	63.8	48.2	34.0	68.3	53.1	36.0
Backward-25	61.6	49.1	33.0	64.6	48.3	34.5	68.7	53.8	35.9
Backward-50	64.2	49.3	32.5	66.3	47.8	34.0	70.8	52.5	36.1

From Table 1, we find that a specific method, e.g., Softmax, performs quite similarly on the many-, medium- and few-shot class subsets even though the test class distributions change significantly. We call this issue *simulation bias*, i.e., their trained model seeks to simulate a specific class distribution without adaptation. For example, the model obtained from the softmax loss simulates the original long-tailed training distribution, and it performs the worst on the few-shot subset even though the test class distribution is backward long-tailed. In contrast, the models trained by existing long-tailed recognition methods try to simulate a more balanced test class distribution. More critically, when the test class distribution varies, the simulation bias does not adapt and keeps unchanged. As a result, despite performing well on the uniform test class distributions, existing methods cannot adapt to other distributions well (c.f. Table 9).

Method overview From the above results, we observe that the models learned by different approaches are good at dealing with different test class distributions. To leverage their individual advantage, we propose a novel method to handle test-agnostic long-tailed recognition, namely Test-time Aggregating Diverse Experts (TADE). TADE introduces two solution strategies: (1) learning skill-diverse experts to constitute a multi-expert model from long-tailed training data; and (2) test-time self-supervised aggregation for learning a suitable scheme for aggregating experts. With these two strategies, TADE can deal with arbitrary unknown test class distribution well, providing a better choice for deployment in real-world long-tailed recognition applications.

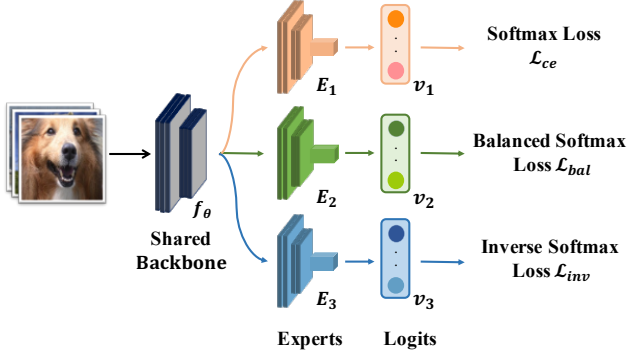


Figure 2. The scheme of TADE with three experts, where different experts are trained with different expertise-guided losses.

4.2. Skill-Diverse Expert Learning

Spectrum-spanned multi-expert framework TADE builds a three-expert model¹, where different experts are trained to be skilled in different class distributions, and integrately span a wide spectrum of possible class distributions. As shown in Figure 2, the three-expert model comprises two components: (1) an expert-shared backbone f_θ ; (2) independent expert networks E_1 , E_2 and E_3 .

Without loss of generality, we take ResNet [15] as an example to illustrate the multi-expert model. Since the shallow layers in deep networks extract more general representations and deeper layers extract more task-specific features [43], the three-expert model uses the first two stages of ResNet as the expert-shared backbone. The later stages of ResNet and the fully-connected layer constitute independent components of each expert, where the number of filters in each expert is reduced by 1/4. By sharing the backbone and using fewer filters in each expert, the computational complexity² of the three-expert model would be reduced [36, 51]. The final prediction is the arithmetic mean on prediction logits of these experts, followed by a softmax function. In order to learn skill-diverse experts, TADE trains each expert with different learning objectives as follows.

Expertise-guided losses As shown in Figure 1(b), the three experts are trained to be skilled in different test class distributions. The forward expert E_1 seeks to be good at the long-tailed distribution as training data and performs well on many-shot classes. The uniform expert E_2 aims to excel at the uniform distribution. The backward expert E_3 strives to be skilled in the inversely long-tailed distribution and performs well on few-shot classes. Here, the forward and backward experts are necessary since they span a wide spectrum of possible class distributions, while the uniform expert ensures that we retain high accuracy on the uniform class distribution. To this end, we use three different expertise-guided loss functions to train experts, respectively.

¹See discussions on the number of experts in Appendix E.1.

²More discussion on the model complexity can be found in Appendix G.

For **the forward expert** E_1 , we directly use the softmax cross-entropy loss to train the expert so that it can simulate the original long-tailed training distribution:

$$\mathcal{L}_{ce} = \frac{1}{n_s} \sum_{x_i \in \mathcal{D}_s} -y_i \log \sigma(v_1(x_i)), \quad (1)$$

where $v_1(\cdot)$ is the output logits of the forward expert, while $\sigma(\cdot)$ is the softmax function.

For **the uniform expert** E_2 , we aim to train the expert to simulate the uniform class distribution. Inspired by the effectiveness of logit adjusted loss for long-tailed recognition [26], we resort to the balanced softmax loss [19]. To be specific, let $\hat{y}^k = p(y=k|x) = \frac{\exp(v^k)}{\sum_{c=1}^C \exp(v^c)}$ be the conditional prediction probability. From the Bayes' theorem, the prediction probability can be interpreted as $p(y=k|x) = \frac{p(x|y=k)p(y=k)}{p(x)}$. In long-tailed recognition, $p(x)$ are generally assumed to be consistent, and the key challenge lies in the class distribution shift, *i.e.*, $p_s(y) \neq p_t(y)$. For training a model to simulate the uniform distribution $p(y=k) = \frac{1}{C}$, we adjust the prediction probability by compensating the long-tailed training class distribution with the training data prior $\pi = p_s(y)$ [19]:

$$\hat{y}^k = \frac{\pi^k \exp(v^k)}{\sum_{c=1}^C \pi^c \exp(v^c)} = \frac{\exp(v^k + \log \pi^k)}{\sum_{c=1}^C \exp(v^c + \log \pi^c)}, \quad (2)$$

where $\pi^k = p_s(y=k) = \frac{n_k}{n}$ denotes the frequency of the training class k . Then the balanced softmax loss is defined as:

$$\mathcal{L}_{bal} = \frac{1}{n_s} \sum_{x_i \in \mathcal{D}_s} -y_i \log \sigma(v_2(x_i) + \log \pi), \quad (3)$$

where $v_2(\cdot)$ denotes the output logits of the uniform expert E_2 . More intuitively, based on logit adjustment to compensate the long-tailed training distribution with the training prior π , this loss enables E_2 to output class-balanced prediction that simulates the uniform class distribution.

For **the backward expert** E_3 , we seek to train it to simulate the inversely long-tailed distribution to the training data. To this end, we follow the same idea of logit adjusted loss and adjust the prediction probability in the softmax loss by:

$$\hat{y}^k = \frac{\exp(v^k + \log \pi^k - \log \bar{\pi}^k)}{\sum_{c=1}^C \exp(v^c + \log \pi^c - \log \bar{\pi}^c)}, \quad (4)$$

where the inverse training prior $\bar{\pi}$ is obtained by inverting the training class distribution, *e.g.*, $\bar{\pi}_1 = \pi_C$. We then propose a new inverse softmax loss to train the backward expert:

$$\mathcal{L}_{inv} = \frac{1}{n_s} \sum_{x_i \in \mathcal{D}_s} -y_i \log \sigma(v_3(x_i) + \log \pi - \lambda \log \bar{\pi}), \quad (5)$$

where λ is a hyper-parameter. Intuitively, based on logit adjustment to compensate the long-tailed distribution with π and adding the inverse long-tailed distribution with $\bar{\pi}$, this loss enables E_3 to simulate the inversely long-tailed distribution well (please refer to Table 4 for empirical verification).

Table 2. Prediction stability of experts in terms of the cosine similarity between predictions of a sample’s two views. Note that expert E_1 is good at many-shot classes and expert E_3 is skilled in few-shot classes. The results show that stronger experts are more stable in the predictions of different views of the data from their skilled classes. Here, the imbalance ratio of CIFAR100-LT is 100.

Object	Cosine similarity between view predictions					
	ImageNet-LT			CIFAR100-LT		
	Many	Med.	Few	Many	Med.	Few
Expert E_1	0.60	0.48	0.43	0.28	0.22	0.20
Expert E_2	0.56	0.50	0.45	0.25	0.21	0.19
Expert E_3	0.52	0.53	0.58	0.22	0.23	0.25

4.3. Test-Time Self-Supervised Aggregation

Based on the skill-diverse learning strategy, the three experts in TADE are skilled in different classes (See Table 4). The remaining question is how to aggregate them to deal with unknown test class distributions.

A basic principle for expert aggregation is that the experts should play a bigger role in situations where they have expertise. Nevertheless, how to detect strong experts for various (unknown) test class distribution remains unknown. Our key insight is that strong experts should be more stable in predicting the samples from their skilled classes, even though these samples are perturbed. To verify this, we estimate the prediction stability of experts by comparing the cosine similarity between their predictions for a sample’s two augmented views. The data views are generated by the same data augmentation techniques as MoCo v2 [5]. Table 2 shows *the positive correlation between expertise and stability* that stronger experts have higher prediction similarity between different views of samples from their favorable class distribution. Following this finding, we propose to explore the relative prediction stability to detect strong experts and weight different experts for test class distributions.

Prediction stability maximization Based on the above motivation, we design a novel self-supervised method, namely prediction stability maximization. The method seeks to learn aggregation weights for each expert (frozen parameters) by maximizing mode prediction stability for unlabeled test samples. As shown in Figure 3, the method comprises three major components: data view generation, aggregation weight and prediction stability loss.

Data View generation For a given sample x , we conduct two stochastic data augmentations to generate the sample’s two views, *i.e.*, x_1 and x_2 . Here, we use the same data augmentation techniques as the advanced contrastive self-supervised learning method, *i.e.*, MoCo v2 [5].

Aggregation weights Given the output logits of three experts $(v_1, v_2, v_3) \in \mathbb{R}^{3 \times C}$, we aggregate experts with an aggregation weight $w = [w_1, w_2, w_3] \in \mathbb{R}^3$ and obtain the final softmax prediction by $\hat{y} = \sigma(w_1 \cdot v_1 + w_2 \cdot v_2 + w_3 \cdot v_3)$, where w is normalized before aggregation, *i.e.*, $w_1 + w_2 + w_3 = 1$.

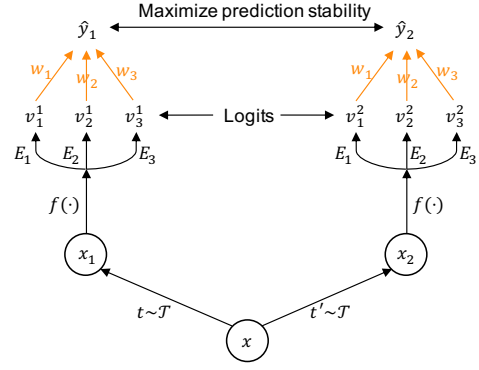


Figure 3. The scheme of test-time self-supervised aggregation. Two data augmentations sampled from the same family of augmentations ($t \sim \mathcal{T}$ and $t' \sim \mathcal{T}$) are applied to obtain two data views.

Prediction stability loss Given the view predictions of all test data, we maximize the prediction stability based on the cosine similarity between the view predictions:

$$\max_w \mathcal{L}_{sta} = \frac{1}{n_t} \sum_{x \in \mathcal{D}_t} \hat{y}_1^\top \hat{y}_2, \quad (6)$$

where \hat{y}_1, \hat{y}_2 are normalized by the softmax function. In test-time training, only the aggregation weight w is updated. Since stronger experts have higher prediction similarity for their skilled classes, maximizing \mathcal{L}_{sta} would learn higher weights for stronger experts regarding the unknown test distribution. Moreover, to avoid the weight for some weak expert becomes zero, we give a stop condition: if the weight for one expert is less than 0.05, we stop test-time training.

4.4. Theoretical Analysis

In this section, we analyze what the prediction stability maximization strategy tends to learn. To this end, we first define the random variables of predictions and labels as $\hat{Y} \sim p(\hat{y})$ and $Y \sim p_t(y)$. We have the following result:

Theorem 1. *Assuming the data augmentations are strong enough to generate representative data views, then the prediction stability loss \mathcal{L}_{sta} is positive proportional to the mutual information between the prediction distribution and the test class distribution $I(\hat{Y}; Y)$, and negative proportional to the prediction entropy $H(\hat{Y})$:*

$$\mathcal{L}_{sta} \propto I(\hat{Y}; Y) - H(\hat{Y})$$

Please see Appendix A for proofs. According to Theorem 1, maximizing \mathcal{L}_{sta} enables TADE to learn an aggregation weight that maximizes the mutual information between the prediction distribution $p(\hat{y})$ and the test class distribution $p_t(y)$, as well as minimizing the prediction entropy. Since minimizing entropy improves the confidence of the classifier output [11], the aggregation weight is learned to simulate the test class distribution $p_t(y)$ and increase the prediction confidence. Such a property verifies the effectiveness of the proposed method for test-agnostic long-tailed recognition. We provide the algorithm pseudo-code in Appendix B.

5. Experiments

We first evaluate the effectiveness of the two strategies in TADE, *i.e.*, skill-diverse expert learning and test-time self-supervised learning. We then evaluate the performance of TADE on vanilla and test-agnostic long-tailed recognition.

5.1. Experimental Setups

Datasets We use four benchmark datasets (*i.e.*, ImageNet-LT [24], CIFAR100-LT [2], Places-LT [24], iNaturalist 2018 [32]) to simulate real-world long-tailed data distributions. The imbalance ratio is defined as $\max n_j / \min n_j$, where n_j denotes the sample number of class j . Among them, CIFAR100-LT has three variants with different imbalance ratios. The dataset statistics are summarized in Table 3.

Table 3. Statistics of datasets.

Dataset	# classes	# training data	# test data	imbalance ratio
ImageNet-LT [24]	1,000	115,846	50,000	256
CIFAR100-LT [2]	100	50,000	10,000	{10,50,100}
Places-LT [24]	365	625,000	36,500	996
iNaturalist 2018 [32]	8,142	437,513	24,426	500

Baselines We compare TADE with state-of-the-art long-tailed methods, including two-stage based methods (Decouple [22], MiSLAS [50]), logit-adjusted training (Balanced Softmax [19], LADE [16]), ensemble learning (BBN [51], RIDE (with 3 experts) [36]), classifier design (Causal [30]), and representation learning (KCL [21]). Note that LADE assumes the prior of the test class distribution is accessible, while all other methods do not use any test prior.

Evaluation protocols We consider two evaluation protocols: the conventional one and the test-agnostic one. In the conventional protocol [22, 24], the models are evaluated on the uniform test class distribution in terms of top-1 accuracy. We also report accuracy on three groups of classes: Many-shot (more than 100 images), Medium-shot (20~100 images) and Few-shot (less than 20 images). In the test-agnostic protocol, the models are evaluated on multiple sets of test samples, following different class distributions, in terms of top-1 accuracy. Following [16], we construct three kinds of test class distributions, *i.e.*, the uniform distribution, forward long-tailed distributions as training data, and backward long-tailed distributions. In the backward one, the long-tailed order of classes is flipped. More details of test data construction are put in Appendix C.1.

Implementation details We implement all experiments in PyTorch. Following [16, 36], we use ResNeXt-50 for ImageNet-LT, ResNet-32 for CIFAR100-LT, ResNet-152 for Places-LT and ResNet-50 for iNaturalist 2018 as backbones. If not specified, we use SGD optimizer with momentum 0.9 and learning rate 0.1 (linear decay). Moreover, we set $\lambda=2$ for ImageNet-LT and CIFAR100-LT, and $\lambda=1$ for another two datasets. In test-time training, we train the aggregation weights for 5 epochs. More details are put in Appendix C.2.

Table 4. Performance of each expert on the uniform test distribution. Here, the training imbalance ratio of CIFAR100-LT is 100.

Object	RIDE [36]							
	ImageNet-LT				CIFAR100-LT			
	Many	Med.	Few	All	Many	Med.	Few	All
Expert E_1	64.3	49.0	31.9	52.6	63.5	44.8	20.3	44.0
Expert E_2	64.7	49.4	31.2	52.8	63.1	44.7	20.2	43.8
Expert E_3	64.3	48.9	31.8	52.5	63.9	45.1	20.5	44.3
Ensemble	68.0	52.9	35.1	56.3	67.4	49.5	23.7	48.0

Object	TADE (ours)							
	ImageNet-LT				CIFAR100-LT			
	Many	Med.	Few	All	Many	Med.	Few	All
Expert E_1	68.8	43.7	17.2	49.8	67.6	36.3	6.8	38.4
Expert E_2	65.5	50.5	33.3	53.9	61.2	44.7	23.5	44.2
Expert E_3	43.4	48.6	53.9	47.3	14.0	27.6	41.2	25.8
Ensemble	67.0	56.7	42.6	58.8	61.6	50.5	33.9	49.4

Table 5. The learned aggregation weights by our test-time self-supervised learning strategy under different test class distributions.

Test Dist.	ImageNet-LT		
	Expert E_1 (w_1)	Expert E_2 (w_2)	Expert E_3 (w_3)
Forward-50	0.52	0.35	0.13
Forward-10	0.46	0.36	0.18
Uniform	0.33	0.33	0.34
Backward-10	0.21	0.29	0.50
Backward-50	0.17	0.27	0.56

5.2. Effectiveness of Skill-Diverse Expert Learning

This section examines the skill-diverse expert learning strategy. We report the results in Table 4, where RIDE [36] is the state-of-the-art ensemble-based method. Specifically, RIDE trains each expert with cross-entropy independently and uses a KL-Divergence based loss to improve the diversity of each expert. However, simply maximizing the divergence of expert prediction cannot learn visibly diverse experts, as shown in Table 4. In contrast, the three experts trained by our expertise-guided losses learn very different expertise, excelling at many-shot classes, the uniform class distribution (with higher overall performance), and few-shot classes, respectively. The increasing expert diversity further enhances the performance of ensemble learning, which demonstrates the effectiveness of our skill-diverse expert learning strategy. More detailed results are put in Appendix D.1.

5.3. Effectiveness of Test-Time Expert Aggregation

As shown in Table 5, our test-time self-supervised aggregation method can learn suitable expert weights for diverse test class distributions. For the forward long-tailed distribution, the weight for the forward expert E_1 is higher, while for the backward long-tailed distribution, the weight of the backward expert E_3 is relatively high. As a result, our method enhances the performance of the dominant test classes in arbitrary test class distributions, leading to better overall performance (c.f. Table 6). Moreover, when the test dataset gets more imbalanced, the performance gain would be more significant. More results are put in Appendix D.2.

Table 6. The performance improvement via test-time self-supervised learning under diverse test class distributions on ImageNet-LT.

Test Dist.	ImageNet-LT							
	Ours w/o test-time learning				Ours w/ test-time learning			
	Many	Med.	Few	All	Many	Med.	Few	All
Forward-50	65.6	55.7	44.1	65.5	70.0	53.2	33.1	69.4 (+3.9)
Forward-10	66.5	56.8	44.2	63.6	69.9	54.3	34.7	65.4 (+1.8)
Uniform	67.0	56.7	42.6	58.8	66.5	57.0	43.5	58.8 (+0.0)
Backward-10	65.0	57.6	43.1	53.1	60.9	57.5	50.1	54.5 (+1.4)
Backward-50	69.1	57.0	42.9	49.8	60.7	56.2	50.7	53.1 (+3.3)

Table 7. Top-1 accuracy on ImageNet-LT.

Method	Many	Med.	Few	All
Softmax	68.1	41.5	14.0	48.0
Decouple-LWS [22]	61.8	47.6	30.9	50.8
Causal [30]	64.1	45.8	27.2	50.3
Balanced Softmax [19]	64.1	48.2	33.4	52.3
KCL [21]	61.8	45.9	27.3	49.5
MiSLAS [50]	62.0	49.1	32.8	51.4
LADE [16]	64.4	47.7	34.3	52.3
RIDE [36]	68.0	52.9	35.1	56.3
TADE (ours)	66.5	57.0	43.5	58.8

Table 8. Top-1 accuracy on CIFAR100-LT, Places-LT and iNaturalist 2018, where the test class distribution is uniform. More results on three groups of classes are put in Appendix.

(a) CIFAR100-LT				(b) Places-LT		(c) iNaturalist 2018	
Imbalance Ratio	10	50	100	Method	Top-1 accuracy	Method	Top-1 accuracy
Softmax	59.1	45.6	41.4	Softmax	31.4	Softmax	64.7
BBN [51]	59.8	49.3	44.7	Causal [30]	32.2	Causal [30]	64.4
Causal [30]	59.4	48.8	45.0	Balanced Softmax [19]	39.4	Balanced Softmax [19]	70.6
Balanced Softmax [19]	61.0	50.9	46.1	MiSLAS [50]	38.3	MiSLAS [50]	70.7
MiSLAS [50]	62.5	51.5	46.8	LADE [16]	39.2	LADE [16]	69.3
LADE [16]	61.6	50.1	45.6	RIDE [36]	40.3	RIDE [36]	71.8
RIDE [36]	61.8	51.7	48.0	TADE (ours)	40.9	TADE (ours)	72.9
TADE (ours)	63.6	53.9	49.8				

5.4. Results on Uniform Test Class Distribution

This section compares the proposed TADE with state-of-the-art long-tailed recognition methods on four benchmark datasets under the uniform test class distribution.

ImageNet-LT We train models for 180 epochs with cosine learning rate decay. The batch size for most baselines is 256 (learning rate 0.1), while that for RIDE and our method is 64 (learning rate 0.025). The results are reported in Table 7. Softmax trains the model with cross-entropy, so it simulates the training class distribution and performs quite well on many-shot classes. However, it performs relatively bad on medium-shot and few-shot classes, leading to worse overall performance. In contrast, existing long-tailed recognition methods (*e.g.*, Decouple, Causal, Balanced Softmax) seek to simulate the uniform test class distribution, and thus their performance on the three groups of classes are more balanced, leading to better overall performance. However, since these methods mainly seek balanced performance, they inevitably sacrifice the performance on many-shot classes. To address this issue, RIDE explores ensemble learning for long-tailed recognition, and achieves better performance on tail classes without sacrificing the performance on head classes a lot. In comparison, based on the increasing expert diversity derived from skill-diverse expert learning, our method performs state-of-the-art on ImageNet-LT, with 2.5 performance improvement than RIDE. Such results demonstrate the superiority of TADE over compared methods.

CIFAR100-LT We train all methods for 200 epochs with batch size 128. The results are reported in Table 8 (a), where all long-tailed recognition methods perform better than Softmax. For these compared methods, one interesting observation is that RIDE outperforms all other baselines significantly under the imbalance ratio 100, but it performs worse than MiSLAS under the imbalance ratio 10. This means when the imbalance ratio of the long-tailed data is relatively low, the effectiveness of naive ensemble learning to handle class imbalance is less competitive than data augmentation. Even so, LADE performs the best on CIFAR100-LT under all imbalance ratios (including the imbalance ratio 10), which further verifies the value of skill-diverse expert learning.

Places-LT Following [22, 24], we use ResNet-152 pre-trained on ImageNet as the backbone. The batch size is 128 and the learning rate is 0.01. The training epoch for MiSLAS is 100, and that for all other methods is 30. The results in Table 8 (b) show that our proposed method also achieves the best performance on Places-LT.

iNaturalist 2018 We train most baselines for 200 epochs with batch size 256 and learning rate 0.1. For RIDE and our method, we adjust the batch size to 512 and the learning rate to 0.2. As shown in Table 8 (c), the proposed method achieves new state-of-the-art performance, *i.e.*, 40.9 top-1 accuracy. Such results demonstrate that TADE handles highly imbalanced fine-grained image data well, even though there are a very large number of classes.

Table 9. Top-1 accuracy over all classes under diverse unknown test class distributions. ‘‘Prior’’ indicates that the test class distribution is used as prior knowledge. ‘‘Uni.’’ denotes the uniform distribution. ‘‘IR’’ indicates the imbalance ratio. ‘‘BS’’ denotes the balanced softmax [19].

		(a) ImageNet-LT										(b) CIFAR100 (IR10)											
Method	Prior	Forward					Uni.	Backward					Forward					Uni.	Backward				
		50	25	10	5	2	1	2	5	10	25	50	50	25	10	5	2	1	2	5	10	25	50
Softmax	✗	66.1	63.8	60.3	56.6	52.0	48.0	43.9	38.6	34.9	30.9	27.6	72.0	69.6	66.4	65.0	61.2	59.1	56.3	53.5	50.5	48.7	46.5
BS	✗	63.2	61.9	59.5	57.2	54.4	52.3	50.0	47.0	45.0	42.3	40.8	65.9	64.9	64.1	63.4	61.8	61.0	60.0	58.2	57.5	56.2	55.1
MiSLAS	✗	61.6	60.4	58.0	56.3	53.7	51.4	49.2	46.1	44.0	41.5	39.5	67.0	66.1	65.5	64.4	63.2	62.5	61.2	60.4	59.3	58.5	57.7
LADE	✗	63.4	62.1	59.9	57.4	54.6	52.3	49.9	46.8	44.9	42.7	40.7	67.5	65.8	65.8	64.4	62.7	61.6	60.5	58.8	58.3	57.4	57.7
LADE	✓	65.8	63.8	60.6	57.5	54.5	52.3	50.4	48.8	48.6	49.0	49.2	71.2	69.3	67.1	64.6	62.4	61.6	60.4	61.4	61.5	62.7	64.8
RIDE	✗	67.6	66.3	64.0	61.7	58.9	56.3	54.0	51.0	48.7	46.2	44.0	67.1	65.3	63.6	62.1	60.9	61.8	58.4	56.8	55.3	54.9	53.4
TADE	✗	69.4	67.4	65.4	63.0	60.6	58.8	57.1	55.5	54.5	53.7	53.1	71.2	69.4	67.6	66.3	64.4	63.6	62.9	62.4	61.7	62.1	63.0

		(c) CIFAR100 (IR50)										(d) CIFAR100 (IR100)											
Method	Prior	Forward					Uni.	Backward					Forward					Uni.	Backward				
		50	25	10	5	2	1	2	5	10	25	50	50	25	10	5	2	1	2	5	10	25	50
Softmax	✗	64.8	62.7	58.5	55.0	49.9	45.6	40.9	36.2	32.1	26.6	24.6	63.3	62.0	56.2	52.5	46.4	41.4	36.5	30.5	25.8	21.7	17.5
BS	✗	61.6	60.2	58.4	55.9	53.7	50.9	48.5	45.7	43.9	42.5	40.6	57.8	55.5	54.2	52.0	48.7	46.1	43.6	40.8	38.4	36.3	33.7
MiSLAS	✗	60.1	58.9	57.7	56.2	53.7	51.5	48.7	46.5	44.3	41.8	40.2	58.8	57.2	55.2	53.0	49.6	46.8	43.6	40.1	37.7	33.9	32.1
LADE	✗	61.3	60.2	56.9	54.3	52.3	50.1	47.8	45.7	44.0	41.8	40.5	56.0	55.5	52.8	51.0	48.0	45.6	43.2	40.0	38.3	35.5	34.0
LADE	✓	65.9	62.1	58.8	56.0	52.3	50.1	48.3	45.5	46.5	46.8	47.8	62.6	60.2	55.6	52.7	48.2	45.6	43.8	41.1	41.5	40.7	41.6
RIDE	✗	62.2	61.0	58.8	56.4	52.9	51.7	47.1	44.0	41.4	38.7	37.1	63.0	59.9	57.0	53.6	49.4	48.0	42.5	38.1	35.4	31.6	29.2
TADE	✗	67.2	64.5	61.2	58.6	55.4	53.9	51.9	50.9	51.0	51.7	52.8	65.9	62.5	58.3	54.8	51.1	49.8	46.2	44.7	43.9	42.5	42.4

		(e) Places-LT										(f) iNaturalist 2018					
Method	Prior	Forward					Uni.	Backward					Forward		Uni.	Backward	
		50	25	10	5	2	1	2	5	10	25	50	3	2	1	2	3
Softmax	✗	45.6	42.7	40.2	38.0	34.1	31.4	28.4	25.4	23.4	20.8	19.4	65.4	65.5	64.7	64.0	63.4
BS	✗	42.7	41.7	41.3	41.0	40.0	39.4	38.5	37.8	37.1	36.2	35.6	70.3	70.5	70.6	70.6	70.8
MiSLAS	✗	40.9	39.7	39.5	39.6	38.8	38.3	37.3	36.7	35.8	34.7	34.4	70.8	70.8	70.7	70.7	70.2
LADE	✗	42.8	41.5	41.2	40.8	39.8	39.2	38.1	37.6	36.9	36.0	35.7	68.4	69.0	69.3	69.6	69.5
LADE	✓	46.3	44.2	42.2	41.2	39.7	39.4	39.2	39.9	40.9	42.4	43.0	✗	69.1	69.3	70.2	✗
RIDE	✗	43.1	41.8	41.6	42.0	41.0	40.3	39.6	38.7	38.2	37.0	36.9	71.5	71.9	71.8	71.9	71.8
TADE	✗	46.4	44.9	43.3	42.6	41.3	40.9	40.6	41.1	41.4	42.0	41.6	72.3	72.5	72.9	73.5	73.3

5.5. Results on Diverse Test Class Distributions

This section compares the proposed method with state-of-the-art long-tailed recognition methods on four benchmark datasets with diverse (agnostic) test class distributions.

ImageNet-LT We report the results in Table 9 (a). To be specific, since Softmax seeks to simulate the long-tailed training distribution, it performs well on forward long-tailed test class distributions. However, its performance on the uniform and backward long-tailed distributions is poor. In contrast, existing long-tailed recognition methods show more balanced performance across classes, leading to better overall accuracy. However, the resulting models by these methods suffer from a simulation bias, *i.e.*, performing similarly across classes on different test class distributions (c.f. Table 1). As a result, they cannot adapt to diverse test class distributions well.

To address this task, LADE exploits the prior of test class distributions to adjust model prediction, and thus adapts to different test distributions better. In contrast, our proposed method applies the self-supervised expert aggregation strategy to deal with unknown class distribution (c.f. Table 6), without the need to use any test prior. Considering it is difficult to obtain the test prior in real-world applications, the promising results demonstrate the effectiveness and practicality of our method. Note that the performance gap becomes larger between TADE and baselines when the test dataset gets more imbalanced.

CIFAR100-LT and Places-LT We report the results in Table 9 (b-e). Most observations are similar to ImageNet-LT. One interesting result is that, when the backward long-tailed distribution is very imbalanced, LADE with the test prior performs the best on CIFAR100-LT (IR10) and Places-LT. This shows the effectiveness of the test prior. In contrast, TADE performs comparably on these distributions without using any test prior.

iNaturalist 2018 We report the results in Table 9 (f). Since the number of original test samples is only 3 on each class in iNaturalist 2018, the number of the constructed test class distributions is less than other datasets. Note that on Forward-3 and Backward-3 distributions, the number of test samples on some classes becomes zero. In such cases, the test prior cannot be used in LADE, since adjusting logits with log 0 results in biased predictions. As shown in Table 9 (f), TADE still achieves state-of-the-art on all test class distributions.

6. Conclusion

This work studies a new task of test-agnostic long-tailed recognition, where the test class distribution is unknown and arbitrary. To address this, we propose a new method, namely Test-time Aggregating Diverse Experts (TADE), with two new solution strategies: skill-diverse expert learning and test-time self-supervised aggregation. We theoretically analyze the proposed method and also empirically show that our method achieves new state-of-the-art performance on both vanilla and test-agnostic long-tailed recognition.

References

- [1] Malik Boudiaf, Jérôme Rony, et al. A unifying mutual information view of metric learning: cross-entropy vs. pairwise losses. In *European Conference on Computer Vision*, 2020. 11
- [2] Kaidi Cao, Colin Wei, Adrien Gaidon, Nikos Arechiga, and Tengyu Ma. Learning imbalanced datasets with label-distribution-aware margin loss. In *Advances in Neural Information Processing Systems*, 2019. 1, 2, 6
- [3] Nitesh V Chawla, Kevin W Bowyer, Lawrence O Hall, and W Philip Kegelmeyer. Smote: synthetic minority over-sampling technique. *Journal of artificial intelligence research*, 16:321–357, 2002. 1, 2
- [4] Ting Chen, Simon Kornblith, Mohammad Norouzi, and Geoffrey Hinton. A simple framework for contrastive learning of visual representations. In *International Conference on Machine Learning*, 2020. 2
- [5] Xinlei Chen, Haoqi Fan, Ross Girshick, and Kaiming He. Improved baselines with momentum contrastive learning. *ArXiv*, 2020. 5, 12
- [6] Xinlei Chen and Kaiming He. Exploring simple siamese representation learning. In *IEEE Computer Vision and Pattern Recognition*, pages 15750–15758, 2021. 2
- [7] Zhixiang Chi, Yang Wang, Yuanhao Yu, and Jin Tang. Test-time fast adaptation for dynamic scene deblurring via meta-auxiliary learning. In *IEEE Computer Vision and Pattern Recognition*, pages 9137–9146, 2021. 2
- [8] Yin Cui, Menglin Jia, Tsung-Yi Lin, Yang Song, and Serge Belongie. Class-balanced loss based on effective number of samples. In *IEEE Computer Vision and Pattern Recognition*, pages 9268–9277, 2019. 1, 2
- [9] Jia Deng, Wei Dong, Richard Socher, Li-Jia Li, Kai Li, and Li Fei-Fei. Imagenet: A large-scale hierarchical image database. In *IEEE Computer Vision and Pattern Recognition*, pages 248–255, 2009. 12
- [10] Zongyong Deng, Hao Liu, Yaoxing Wang, Chenyang Wang, Zekuan Yu, and Xuehong Sun. Pml: Progressive margin loss for long-tailed age classification. In *IEEE Computer Vision and Pattern Recognition*, pages 10503–10512, 2021. 1, 2
- [11] Yves Grandvalet, Yoshua Bengio, et al. Semi-supervised learning by entropy minimization. In *CAP*, pages 281–296, 2005. 5
- [12] Hao Guo and Song Wang. Long-tailed multi-label visual recognition by collaborative training on uniform and re-balanced samplings. In *IEEE Computer Vision and Pattern Recognition*, pages 15089–15098, 2021. 1, 2
- [13] Marton Havasi, Rodolphe Jenatton, Stanislav Fort, Jeremiah Zhe Liu, Jasper Snoek, Balaji Lakshminarayanan, Andrew M Dai, and Dustin Tran. Training independent sub-networks for robust prediction. In *International Conference on Learning Representations*, 2021. 23
- [14] Kaiming He, Haoqi Fan, Yuxin Wu, Saining Xie, and Ross Girshick. Momentum contrast for unsupervised visual representation learning. In *Computer Vision and Pattern Recognition*, 2020. 2
- [15] Kaiming He, Xiangyu Zhang, Shaoqing Ren, and Jian Sun. Deep residual learning for image recognition. In *IEEE Computer Vision and Pattern Recognition*, pages 770–778, 2016. 4
- [16] Youngkyu Hong, Seungju Han, Kwanghee Choi, Seokjun Seo, Beomsu Kim, and Buru Chang. Disentangling label distribution for long-tailed visual recognition. In *IEEE Computer Vision and Pattern Recognition*, 2021. 1, 2, 3, 6, 7, 12, 16
- [17] Chen Huang, Yining Li, Chen Change Loy, and Xiaoou Tang. Learning deep representation for imbalanced classification. In *IEEE Computer Vision and Pattern Recognition*, pages 5375–5384, 2016. 1, 2
- [18] Muhammad Abdullah Jamal, Matthew Brown, Ming-Hsuan Yang, Liqiang Wang, and Boqing Gong. Rethinking class-balanced methods for long-tailed visual recognition from a domain adaptation perspective. In *IEEE Computer Vision and Pattern Recognition*, pages 7610–7619, 2020. 1
- [19] Ren Jiawei, Cunjun Yu, Xiao Ma, Haiyu Zhao, Shuai Yi, et al. Balanced meta-softmax for long-tailed visual recognition. In *Advances in Neural Information Processing Systems*, 2020. 1, 2, 3, 4, 6, 7, 8, 16
- [20] Mohammad Mahdi Kamani, Sadegh Farhang, Mehrdad Mahdavi, and James Z Wang. Targeted data-driven regularization for out-of-distribution generalization. In *ACM SIGKDD International Conference on Knowledge Discovery & Data Mining*, pages 882–891, 2020. 2
- [21] Bingyi Kang, Yu Li, Sa Xie, Zehuan Yuan, and Jiashi Feng. Exploring balanced feature spaces for representation learning. In *International Conference on Learning Representations*, 2021. 1, 2, 6, 7
- [22] Bingyi Kang, Saining Xie, Marcus Rohrbach, Zhicheng Yan, Albert Gordo, Jiashi Feng, and Yannis Kalantidis. Decoupling representation and classifier for long-tailed recognition. In *International Conference on Learning Representations*, 2019. 1, 2, 3, 6, 7, 12
- [23] Yu Li, Tao Wang, Bingyi Kang, Sheng Tang, Chunfeng Wang, Jintao Li, and Jiashi Feng. Overcoming classifier imbalance for long-tail object detection with balanced group softmax. In *IEEE Computer Vision and Pattern Recognition*, pages 10991–11000, 2020. 1, 2
- [24] Ziwei Liu, Zhongqi Miao, Xiaohang Zhan, Jiayun Wang, Boqing Gong, and Stella X Yu. Large-scale long-tailed recognition in an open world. In *IEEE Computer Vision and Pattern Recognition*, pages 2537–2546, 2019. 1, 6, 7, 12
- [25] Mingsheng Long, Jianmin Wang, Guiguang Ding, Jianguang Sun, and Philip S Yu. Transfer joint matching for unsupervised domain adaptation. In *IEEE Computer Vision and Pattern Recognition*, pages 1410–1417, 2014. 2
- [26] Aditya Krishna Menon, Sadeep Jayasumana, Ankit Singh Rawat, Himanshu Jain, Andreas Veit, and Sanjiv Kumar. Long-tail learning via logit adjustment. In *International Conference on Learning Representations*, 2021. 1, 2, 4
- [27] Prashant Pandey, Mrigank Raman, Sumanth Varambally, and Prathosh AP. Generalization on unseen domains via inference-time label-preserving target projections. In *IEEE Computer Vision and Pattern Recognition*, pages 12924–12933, 2021. 2
- [28] Yu Sun, Xiaolong Wang, Zhuang Liu, John Miller, Alexei Efros, and Moritz Hardt. Test-time training with self-supervision for generalization under distribution shifts. In

- International Conference on Machine Learning*, pages 9229–9248. PMLR, 2020. [2](#)
- [29] Jingru Tan, Changbao Wang, Buyu Li, Quanquan Li, Wanli Ouyang, Changqing Yin, and Junjie Yan. Equalization loss for long-tailed object recognition. In *IEEE Computer Vision and Pattern Recognition*, pages 11662–11671, 2020. [1](#), [2](#)
- [30] Kaihua Tang, Jianqiang Huang, and Hanwang Zhang. Long-tailed classification by keeping the good and removing the bad momentum causal effect. *Advances in Neural Information Processing Systems*, 33, 2020. [6](#), [7](#), [16](#)
- [31] Junjiao Tian, Yen-Cheng Liu, Nathan Glaser, Yen-Chang Hsu, and Zsolt Kira. Posterior re-calibration for imbalanced datasets. In *Advances in Neural Information Processing Systems*, 2020. [2](#)
- [32] Grant Van Horn, Oisín Mac Aodha, Yang Song, Yin Cui, Chen Sun, Alex Shepard, Hartwig Adam, Pietro Perona, and Serge Belongie. The inaturalist species classification and detection dataset. In *IEEE Computer Vision and Pattern Recognition*, pages 8769–8778, 2018. [6](#)
- [33] Thomas Varsavsky, Mauricio Orbes-Arteaga, Carole H Sudre, Mark S Graham, Parashkev Nachev, and M Jorge Cardoso. Test-time unsupervised domain adaptation. In *International Conference on Medical Image Computing and Computer-Assisted Intervention*, pages 428–436, 2020. [2](#)
- [34] Jiaqi Wang, Wenwei Zhang, Yuhang Zang, Yuhang Cao, Jiangmiao Pang, Tao Gong, Kai Chen, Ziwei Liu, Chen Change Loy, and Dahua Lin. Seesaw loss for long-tailed instance segmentation. In *IEEE Computer Vision and Pattern Recognition*, pages 9695–9704, 2021. [1](#)
- [35] Peng Wang, Kai Han, Xiu-Shen Wei, Lei Zhang, and Lei Wang. Contrastive learning based hybrid networks for long-tailed image classification. In *IEEE Computer Vision and Pattern Recognition*, pages 943–952, 2021. [2](#)
- [36] Xudong Wang, Long Lian, Zhongqi Miao, Ziwei Liu, and Stella X Yu. Long-tailed recognition by routing diverse distribution-aware experts. In *International Conference on Learning Representations*, 2021. [1](#), [2](#), [3](#), [4](#), [6](#), [7](#), [12](#), [13](#), [16](#), [23](#)
- [37] Yeming Wen, Dustin Tran, and Jimmy Ba. Batchensemble: an alternative approach to efficient ensemble and lifelong learning. In *International Conference on Learning Representations*, 2020. [23](#)
- [38] Yandong Wen, Kaipeng Zhang, Zhifeng Li, and Yu Qiao. A discriminative feature learning approach for deep face recognition. In *European Conference on Computer Vision*, pages 499–515, 2016. [11](#)
- [39] Zhenzhen Weng, Mehmet Giray Ogut, Shai Limonchik, and Serena Yeung. Unsupervised discovery of the long-tail in instance segmentation using hierarchical self-supervision. In *IEEE Computer Vision and Pattern Recognition*, pages 2603–2612, 2021. [2](#)
- [40] Zhirong Wu, Yuanjun Xiong, Stella X Yu, and Dahua Lin. Unsupervised feature learning via non-parametric instance discrimination. In *IEEE Computer Vision and Pattern Recognition*, 2018. [2](#)
- [41] Liuyu Xiang, Guiguang Ding, and Jungong Han. Learning from multiple experts: Self-paced knowledge distillation for long-tailed classification. In *European Conference on Computer Vision*, 2020. [1](#), [2](#)
- [42] Yuzhe Yang and Zhi Xu. Rethinking the value of labels for improving class-imbalanced learning. In *Advances in Neural Information Processing Systems*, 2020. [2](#)
- [43] Jason Yosinski, Jeff Clune, Yoshua Bengio, and Hod Lipson. How transferable are features in deep neural networks? In *Advances in Neural Information Processing Systems*, volume 27, pages 3320–3328, 2014. [4](#)
- [44] Songyang Zhang, Zeming Li, Shipeng Yan, Xuming He, and Jian Sun. Distribution alignment: A unified framework for long-tail visual recognition. In *IEEE Computer Vision and Pattern Recognition*, pages 2361–2370, 2021. [1](#)
- [45] Yifan Zhang, Hanbo Chen, Ying Wei, Peilin Zhao, Jiezhong Cao, Xinjuan Fan, Xiaoying Lou, Hailing Liu, Jinlong Hou, Xiao Han, et al. From whole slide imaging to microscopy: Deep microscopy adaptation network for histopathology cancer image classification. In *International Conference on Medical Image Computing and Computer-Assisted Intervention*, pages 360–368. Springer, 2019. [2](#)
- [46] Yifan Zhang, Bryan Hooi, et al. Unleashing the power of contrastive self-supervised visual models via contrast-regularized fine-tuning. *ArXiv*, 2021. [2](#), [11](#)
- [47] Yifan Zhang, Ying Wei, et al. Collaborative unsupervised domain adaptation for medical image diagnosis. *IEEE Transactions on Image Processing*, 2020. [2](#)
- [48] Yifan Zhang, Peilin Zhao, Jiezhong Cao, Wenye Ma, Junzhou Huang, Qingyao Wu, and Mingkui Tan. Online adaptive asymmetric active learning for budgeted imbalanced data. In *ACM SIGKDD International Conference on Knowledge Discovery & Data Mining*, pages 2768–2777, 2018. [2](#)
- [49] Peilin Zhao, Yifan Zhang, Min Wu, Steven CH Hoi, Mingkui Tan, and Junzhou Huang. Adaptive cost-sensitive online classification. *IEEE Transactions on Knowledge and Data Engineering*, 31(2):214–228, 2018. [2](#)
- [50] Zhisheng Zhong, Jiequan Cui, Shu Liu, and Jiaya Jia. Improving calibration for long-tailed recognition. In *IEEE Computer Vision and Pattern Recognition*, 2021. [3](#), [6](#), [7](#), [16](#)
- [51] Boyan Zhou, Quan Cui, Xiu-Shen Wei, and Zhao-Min Chen. Bbn: Bilateral-branch network with cumulative learning for long-tailed visual recognition. In *IEEE Computer Vision and Pattern Recognition*, pages 9719–9728, 2020. [1](#), [2](#), [4](#), [6](#), [7](#)

Appendix

We organize the appendix as follows:

- Appendix A: the proofs for Theorem 1.
- Appendix B: the pseudo-code of the proposed method.
- Appendix C: more experimental settings.
- Appendices D-F: more empirical results.

A. Proofs for Theorem 1

Proof. We first recall notations in the main paper and define some new notations. The random variables of predictions and labels are defined as $\hat{Y} \sim p(\hat{y})$ and $Y \sim p(y)$, respectively. The number of classes is denoted by C . We further denote the test sample set of the class k by \mathcal{Z}_k , in which the total number of samples in this class is denoted by $|\mathcal{Z}_k|$. Let $c_k = \frac{1}{|\mathcal{Z}_k|} \sum_{\hat{y} \in \mathcal{Z}_k} \hat{y}$ represent the hard mean of all predictions of samples from the class k , and let the symbol $\stackrel{c}{=}$ indicate equality up to a multiplicative and/or additive constant.

As shown in Eq.(6), the optimization objective of our test-time self-supervised learning method is to maximize $\mathcal{L}_{sta} = \sum_{j=1}^{n_t} \hat{y}_{j,1}^\top \hat{y}_{j,2}$, where n_t denotes the number of test samples. For convenience, we simplify the first data view to be the original data, so the objective function becomes $\sum_{j=1}^{n_t} \hat{y}_j^\top \hat{y}_{j,2}$. Maximizing such an objective is equivalent to minimizing $\sum_{j=1}^{n_t} -\hat{y}_j^\top \hat{y}_{j,2}$. Here, we assume the data augmentations are strong enough to generate representative data views that can simulate the test data from the same class. In this sense, the new data view can be regarded as an independent sample from the same class. Following this, we analyze our method by connecting $-\hat{y}_j^\top \hat{y}_{j,2}$ to $\sum_{\hat{y}_j \in \mathcal{Z}_k} \|\hat{y}_j - c_k\|^2$, which is similar to the tightness term in the center loss [38]:

$$\begin{aligned}
& \sum_{\hat{y}_j, \hat{y}_{j,2} \in \mathcal{Z}_k} -\hat{y}_j^\top \hat{y}_{j,2} \\
& \stackrel{c}{=} \frac{1}{|\mathcal{Z}_k|} \sum_{\hat{y}_j, \hat{y}_{j,2} \in \mathcal{Z}_k} -\hat{y}_j^\top \hat{y}_{j,2} \\
& \stackrel{c}{=} \frac{1}{|\mathcal{Z}_k|} \sum_{\hat{y}_j, \hat{y}_{j,2} \in \mathcal{Z}_k} \|\hat{y}_j\|^2 - \hat{y}_j^\top \hat{y}_{j,2} \\
& = \sum_{\hat{y}_j \in \mathcal{Z}_k} \|\hat{y}_j\|^2 - \frac{1}{|\mathcal{Z}_k|} \sum_{\hat{y}_j \in \mathcal{Z}_k} \sum_{\hat{y}_{j,2} \in \mathcal{Z}_k} \hat{y}_j^\top \hat{y}_{j,2} \\
& = \sum_{\hat{y}_j \in \mathcal{Z}_k} \|\hat{y}_j\|^2 - 2 \frac{1}{|\mathcal{Z}_k|} \sum_{\hat{y}_j \in \mathcal{Z}_k} \sum_{\hat{y}_{j,2} \in \mathcal{Z}_k} \hat{y}_j^\top \hat{y}_{j,2} \\
& \quad + \frac{1}{|\mathcal{Z}_k|} \sum_{\hat{y}_j \in \mathcal{Z}_k} \sum_{\hat{y}_{j,2} \in \mathcal{Z}_k} \hat{y}_j^\top \hat{y}_{j,2} \\
& = \sum_{\hat{y}_j \in \mathcal{Z}_k} \|\hat{y}_j\|^2 - 2 \hat{y}_j^\top c_k + \|c_k\|^2 \\
& = \sum_{\hat{y}_j \in \mathcal{Z}_k} \|\hat{y}_j - c_k\|^2,
\end{aligned}$$

where we use the property of normalized predictions that $\|\hat{y}_j\|^2 = \|\hat{y}_{j,2}\|^2 = 1$ and the definition of the class hard mean $c_k = \frac{1}{|\mathcal{Z}_k|} \sum_{\hat{y} \in \mathcal{Z}_k} \hat{y}$.

By summing over all classes k , we obtain:

$$\sum_{j=1}^{n_t} -\hat{y}_j^\top \hat{y}_{j,2} \stackrel{c}{=} \sum_{j=1}^{n_t} \|\hat{y}_j - c_{y_i}\|^2.$$

Based on this equation, following [1, 46], we can interpret $\sum_{j=1}^{n_t} -\hat{y}_j^\top \hat{y}_{j,2}$ as a conditional cross-entropy between \hat{Y} and another random variable \bar{Y} , whose conditional distribution given Y is a standard Gaussian centered around c_Y : $\bar{Y}|Y \sim \mathcal{N}(c_Y, i)$:

$$\sum_{j=1}^{n_t} -\hat{y}_j^\top \hat{y}_{j,2} \stackrel{c}{=} \mathcal{H}(\hat{Y}; \bar{Y}|Y) = \mathcal{H}(\hat{Y}|Y) + \mathcal{D}_{KL}(\hat{Y}||\bar{Y}|Y).$$

Hence, we know that $\sum_{j=1}^{n_t} -\hat{y}_j^\top \hat{y}_{j,2}$ is an upper bound on the conditional entropy of predictions \hat{Y} given labels Y :

$$\sum_{j=1}^{n_t} -\hat{y}_j^\top \hat{y}_{j,2} \stackrel{c}{\geq} \mathcal{H}(\hat{Y}|Y).$$

where the symbol $\stackrel{c}{\geq}$ represents “larger than” up to a multiplicative and/or an additive constant. Moreover, when $\hat{Y}|Y \sim \mathcal{N}(c_Y, i)$, the bound is tight. As a result, minimizing $\sum_{j=1}^{n_t} -\hat{y}_j^\top \hat{y}_{j,2}$ is equivalent to minimizing $\mathcal{H}(\hat{Y}|Y)$:

$$\sum_{j=1}^{n_t} -\hat{y}_j^\top \hat{y}_{j,2} \propto \mathcal{H}(\hat{Y}|Y). \quad (7)$$

Meanwhile, the mutual information between predictions \hat{Y} and labels Y can be represented by:

$$\mathcal{I}(\hat{Y}; Y) = \mathcal{H}(\hat{Y}) - \mathcal{H}(\hat{Y}|Y). \quad (8)$$

Combining Eqs.(7-8), we have:

$$\sum_{j=1}^{n_t} -\hat{y}_j^\top \hat{y}_{j,2} \propto -\mathcal{I}(\hat{Y}; Y) + \mathcal{H}(\hat{Y}).$$

Since $\mathcal{L}_{sta} = \sum_{j=1}^{n_t} \hat{y}_j^\top \hat{y}_{j,2}$, we obtain:

$$\mathcal{L}_{sta} \propto \mathcal{I}(\hat{Y}; Y) - \mathcal{H}(\hat{Y}),$$

which concludes the proof for Theorem 1. \square

B. Pseudo-Code

This appendix provides pseudo-code of our proposed TADE method, which consists of two strategies: skill-diverse expert learning and test-time self-supervised aggregation. To be specific, we summarize the skill-diverse expert learning strategy in Algorithm 1 and the test-time self-supervised learning strategy in Algorithm 2. For simplicity, we depict the pseudo-code based on batch size 1, while we conduct batch gradient descent in practice.

Algorithm 1 Skill-diverse Expert Learning

Require: Epochs T ; Hyper-parameters λ for \mathcal{L}_{inv} .**Initialize:** Network backbone f_θ ; Experts E_1, E_2, E_3 .

```
1: for e=1,...,T do
2:   for  $x \in \mathcal{D}_s$  do // batch sampling in practice
3:     Obtain logits  $v_1$  based on  $f_\theta$  and  $E_1$ ;
4:     Obtain logits  $v_2$  based on  $f_\theta$  and  $E_2$ ;
5:     Obtain logits  $v_3$  based on  $f_\theta$  and  $E_3$ ;
6:     Compute loss  $\mathcal{L}_{ce}$  with  $v_1$  for Expert  $E_1$ ; // Eq.(1)
7:     Compute loss  $\mathcal{L}_{bal}$  with  $v_2$  for Expert  $E_2$ ; // Eq.(3)
8:     Compute loss  $\mathcal{L}_{inv}$  with  $v_3$  for Expert  $E_3$ ; // Eq.(5)
9:     loss.backward(). // loss =  $\mathcal{L}_{ce} + \mathcal{L}_{bal} + \mathcal{L}_{inv}$ 
10:  end for
11: end for
return The trained model  $f_\theta, E_1, E_2, E_3$ .
```

Algorithm 2 Test-time Self-supervised Aggregation

Require: Epochs T' ; Trained backbone f_θ ; Trained experts E_1, E_2, E_3 .**Initialize:** Expert aggregation weights w .

```
1: for e=1,...,T' do
2:   for  $x \in \mathcal{D}_t$  do // batch sampling in practice
3:     Draw two augmentation functions  $t \sim \mathcal{T}, t' \sim \mathcal{T}$ ;
4:     Generate data views  $x_1=t(x), x_2=t'(x)$ ;
5:     Obtain logits  $v_1^1, v_2^1, v_3^1$  for the view  $x_1$ ;
6:     Obtain logits  $v_1^2, v_2^2, v_3^2$  for the view  $x_2$ ;
7:     Normalize expert weights  $w$  via softmax function;
8:     Conduct predictions  $\hat{y}_1, \hat{y}_2$  based on  $\hat{y}=wv$ ;
9:     Compute prediction stability loss  $\mathcal{L}_{sta}$ ; // Eq. (6)
10:    Maximize  $\mathcal{L}_{sta}$  to update  $w$ ;
11:  end for
12:  If any  $w_i \leq 0.05$  for  $w_i \in w$ , then stop training.
13: end for
return Expert aggregation weights  $w$ .
```

C. More Experimental Settings

In this appendix, we provide more complete implementation details. We first introduce how to construct distribution-diverse test data sets for each benchmark dataset, followed by more implementation details of our method.

C.1. Constructing Distribution-Agnostic Test Data

Following the construction method in [16], we construct three kinds of test class distributions, *i.e.*, the uniform distribution, forward long-tailed distributions as training data, and backward long-tailed distributions. In the backward ones, the long-tailed class order is flipped. Here, the forward and backward long-tailed test distributions contain multiple different imbalance ratios, *i.e.*, $\rho \in \{2, 5, 10, 25, 50\}$. Although the work [16] only constructs test data for ImageNet-LT, we use the same way to construct distribution-agnostic test datasets for other benchmark datasets, *i.e.*, CIFAR100-LT, Places-LT, iNaturalist 2018.

Considering the long-tailed training categories are sorted by cardinality in decreasing order, the diverse test datasets are constructed as follows: (1) Forward long-tailed distribution: the number of the j -th class is $n_j = N \cdot \rho^{(j-1)/C}$, where N is the sample number per category in the original test dataset and C is the number of classes. (2) Backward long-tailed distribution: the number of the j -th class is $n_j = N \cdot \rho^{(C-j)/C}$. In the backward distributions, the long-tailed order of classes is flipped, so the distribution shift becomes larger with the increase of the imbalance ratio.

For ImageNet-LT, CIFAR100-LT and Places-LT, since there are enough test samples per class, we follow the setting in [16] and construct the imbalance ratio set by $\rho \in \{2, 5, 10, 25, 50\}$. For the iNaturalist 2018 dataset, since there are a very large number of classes, each class only contains three test samples. Therefore, we adjust the imbalance ratio set to $\rho \in \{2, 3\}$ for iNaturalist 2018. Note that, when we set $\rho = 3$, there are some classes in iNaturalist 2018 containing no test sample. All these constructed distribution-agnostic datasets are publicly available along with our code.

C.2. More Implementation Details of Our Method

We implement our method in PyTorch. Following [16, 36], we use ResNeXt-50 for ImageNet-LT, ResNet-32 for CIFAR100-LT, ResNet-152 for Places-LT and ResNet-50 for iNaturalist 2018 as network backbones, while we use the cosine classifier for all datasets.

In the training phase, the data augmentations are the same as existing methods [16, 22]. If not specified, for most datasets, we use the SGD optimizer with momentum 0.9 and initial learning rate 0.1 (linear decay). More specifically, for ImageNet-LT, we train models for 180 epochs with batch size 64 and learning rate 0.025 (cosine decay). For CIFAR100-LT, the training epoch is 200 and the batch size is 128. For Places-LT, following [24, 22], we use ResNet-152 pre-trained on ImageNet [9] as the backbone, where the batch size is 128 and the training epoch is 30. Moreover, the learning rate is 0.01 for the classifier and is 0.001 for all other layers. For iNaturalist 2018, we set the training epoch to 200, the batch size to 512 and the learning rate to 0.2. In the inverse softmax loss, we set $\lambda=2$ for ImageNet-LT and CIFAR100-LT, and set $\lambda=1$ for another two datasets.

In the test-time training, we adopt the same augmentation techniques as MoCo v2 [5] to generate different data views, *i.e.*, random resized crop, color jitter, gray scale, Gaussian blur and horizontal flip. If not specified, we train the aggregation weights for 5 epochs with the same optimizer and learning rate as the training phase. Moreover, the batch size is set to 128 on all datasets.

More detailed statistics of network architectures and hyper-parameters can be found in Table 10. The source code of our method is publicly available at <https://github.com/Vanint/TADE-AgnosticLT>.

Table 10. Statistics of the used network architectures and hyper-parameters in our method.

Items	ImageNet-LT	CIFAR100LT	Places-LT	iNaturalist 2018
Network Architectures				
network backbone	ResNeXt-50	ResNet-32	ResNet-152	ResNet-50
classifier	cosine classifier			
Training Phase				
epochs	180	200	30	200
batch size	64	128	128	512
learning rate (lr)	0.025	0.1	0.01	0.2
lr schedule	cosine decay		linear decay	
λ in inverse softmax loss	2		1	
weight decay factor	5×10^{-4}	5×10^{-4}	4×10^{-4}	2×10^{-4}
momentum factor	0.9			
optimizer	SGD optimizer with nesterov			
Test-time Training				
epochs	5			
batch size	128			
learning rate (lr)	0.025	0.1	0.01	0.1

Table 11. Performance of each expert on the uniform test distribution. Here, the training imbalance ratio of CIFAR100-LT is 100.

Object	RIDE [36]															
	ImageNet-LT				CIFAR100-LT				Places-LT				iNaturalist 2018			
	Many	Med.	Few	All	Many	Med.	Few	All	Many	Med.	Few	All	Many	Med.	Few	All
Expert E_1	64.3	49.0	31.9	52.6	63.5	44.8	20.3	44.0	41.3	40.8	33.2	40.1	66.6	67.1	66.5	66.8
Expert E_2	64.7	49.4	31.2	52.8	63.1	44.7	20.2	43.8	43.0	40.9	33.6	40.3	66.1	67.1	66.6	66.8
Expert E_3	64.3	48.9	31.8	52.5	63.9	45.1	20.5	44.3	42.8	41.0	33.5	40.2	65.3	67.3	66.5	66.7
Ensemble	68.0	52.9	35.1	56.3	67.4	49.5	23.7	48.0	43.2	41.1	33.5	40.3	71.5	72.0	71.6	71.8

Object	TADE (ours)															
	ImageNet-LT				CIFAR100-LT				Places-LT				iNaturalist 2018			
	Many	Med.	Few	All	Many	Med.	Few	All	Many	Med.	Few	All	Many	Med.	Few	All
Expert E_1	68.8	43.7	17.2	49.8	67.6	36.3	6.8	38.4	47.6	27.1	10.3	31.2	76.0	67.1	59.3	66.0
Expert E_2	65.5	50.5	33.3	53.9	61.2	44.7	23.5	44.2	42.6	42.3	32.3	40.5	69.2	70.7	69.8	70.2
Expert E_3	43.4	48.6	53.9	47.3	14.0	27.6	41.2	25.8	22.6	37.2	45.6	33.6	55.6	61.5	72.1	65.1
Ensemble	67.0	56.7	42.6	58.8	61.6	50.5	33.9	49.4	40.4	43.2	36.8	40.9	74.4	72.5	73.1	72.9

D. More Empirical Results

D.1. More Results on Skill-Diverse Expert Learning

This appendix further evaluates the skill-diverse expert learning strategy on CIFAR100-LT, Places-LT and iNaturalist 2018 datasets. We report the results in Table 11, from which we draw the following observations. RIDE [36] is the state-of-the-art ensemble learning based method that tries to learn diverse distribution-aware experts by maximizing the divergence among expert predictions. However, such a method cannot learn visibly diverse experts. As shown in Table 11, where the three experts in RIDE perform very similarly on different groups of classes as well as the overall performance on all benchmark datasets. Such results show that simply maximizing the KL divergence of different experts' predictions is not sufficient to learn very diverse distribution-aware experts.

In contrast, our proposed method learns the skill-diverse experts by directly training each expert with their own corresponding expertise-guided loss. To be specific, the forward expert seeks to learn original long-tailed training distribution, so we directly optimize it with the cross-entropy loss. For the uniform expert, we use the balanced softmax loss to simulate the uniform test distribution. For the backward expert, we design a novel inverse softmax loss to train the expert so that it can simulate the inversely long-tailed distribution to the training data. Table 11 shows that the three experts trained by our method are diverse enough and are skilled in handling different class distributions. Specifically, the forward expert is skilled in many-shot classes, the uniform expert is more balanced with higher overall performance, and the backward expert is good at few-shot classes. Because of such a novel design that enhances expert diversity, our method is able to obtain more promising performance than RIDE.

Table 12. The learned aggregation weights by our test-time self-supervised learning strategy under different test class distributions on ImageNet-LT, CIFAR100-LT, Places-LT and iNaturalist 2018.

Test Dist.	ImageNet-LT			CIFAR100-LT(IR10)			CIFAR100-LT(IR50)		
	E1 (w_1)	E2 (w_2)	E3 (w_3)	E1 (w_1)	E2 (w_2)	E3 (w_3)	E1 (w_1)	E2 (w_2)	E3 (w_3)
Forward-50	0.52	0.35	0.13	0.53	0.38	0.09	0.55	0.38	0.07
Forward-25	0.50	0.35	0.15	0.52	0.37	0.11	0.54	0.38	0.08
Forward-10	0.46	0.36	0.18	0.47	0.36	0.17	0.52	0.37	0.11
Forward-5	0.43	0.34	0.23	0.46	0.34	0.20	0.50	0.36	0.14
Forward-2	0.37	0.35	0.28	0.39	0.37	0.24	0.39	0.38	0.23
Uniform	0.33	0.33	0.34	0.38	0.32	0.3	0.35	0.33	0.33
Backward-2	0.29	0.31	0.40	0.35	0.33	0.31	0.30	0.30	0.40
Backward-5	0.24	0.31	0.45	0.31	0.32	0.37	0.21	0.29	0.50
Backward-10	0.21	0.29	0.50	0.26	0.32	0.42	0.20	0.29	0.51
Backward-25	0.18	0.29	0.53	0.24	0.30	0.46	0.18	0.27	0.55
Backward-50	0.17	0.27	0.56	0.23	0.28	0.49	0.14	0.24	0.62

Test Dist.	CIFAR100-LT(IR100)			Places-LT			iNaturalist 2018		
	E1 (w_1)	E2 (w_2)	E3 (w_3)	E1 (w_1)	E2 (w_2)	E3 (w_3)	E1 (w_1)	E2 (w_2)	E3 (w_3)
Forward-50	0.56	0.38	0.06	0.50	0.20	0.20	-	-	-
Forward-25	0.55	0.38	0.07	0.50	0.20	0.20	-	-	-
Forward-10	0.52	0.39	0.09	0.50	0.20	0.20	-	-	-
Forward-5	0.51	0.37	0.12	0.46	0.32	0.22	-	-	-
Forward-2	0.49	0.35	0.16	0.40	0.34	0.26	0.41	0.34	0.25
Uniform	0.40	0.35	0.24	0.25	0.34	0.41	0.33	0.33	0.34
Backward-2	0.33	0.31	0.36	0.18	0.30	0.52	0.28	0.32	0.40
Backward-5	0.28	0.30	0.42	0.17	0.28	0.55	-	-	-
Backward-10	0.23	0.28	0.49	0.17	0.27	0.56	-	-	-
Backward-25	0.21	0.26	0.53	0.17	0.27	0.56	-	-	-
Backward-50	0.16	0.28	0.56	0.17	0.27	0.56	-	-	-

D.2. More Results on Test-Time Expert Learning

This appendix provides more results to examine the effectiveness of test-time expert aggregation. We report results in Tables 12, from which we draw several observations.

First of all, our method is able to learn suitable expert aggregation weights for arbitrary test class distribution without knowing any test distribution prior. For the forward long-tailed test distribution, where the test sample number of many-shot classes are more than that of medium-shot and few-shot classes, our method learns a higher weight for the forward expert E_1 who is skilled in many-shot classes as well as learning relatively low weights for the expert E_2 and expert E_3 who are good at medium-shot and few-shot classes. Meanwhile, for the uniform test class distribution where all classes have the same number of samples, our test-time expert aggregation strategy learns relatively balanced weights for the three experts. For example, on the uniform ImageNet-LT test data, the learned weights by our strategy are 0.33, 0.33 and 0.34 for each expert, respectively. In addition, for the backward long-tailed test distributions, our method can learn a higher weight for the backward expert E_3 and a relatively low weight for the forward expert E_1 . Note that when the class imbalance ratio becomes larger, our method is able to adaptively learn more diverse expert weights for fitting the actual test class distributions.

Such results not only demonstrate the effectiveness of our strategy, but also verify the theoretical analysis that our method can simulate the unknown test class distribution. To our knowledge, such an ability is quite promising, since it is very difficult to know the practical test class distributions in real-world tasks. This implies that our method is a better candidate to handle real-world long-tailed applications.

Relying on the learned expert weights, our method aggregates the three models appropriately and thus obtain promising performance gain on diverse test class distributions, as shown in Table 13. Note that the performance gain than existing methods is more significant when the test dataset gets more imbalanced. For example, on CIFAR100-LT with the imbalance ratio of 50, our test-time self-supervised aggregation strategy obtains 7.7 performance gain in top-1 accuracy on the forward-50 long-tailed distribution and 9.2 performance gain on the backward-50 long-tailed distribution.

In addition, since the imbalance degrees of the test datasets are relatively low on iNaturalist 2018, the simulated test class distributions are thus relatively balanced. As a result, the obtained performance improvement is not that significant, compared to other datasets. Even so, if there are more iNaturalist test samples following highly imbalanced test class distributions in practical applications, our method can obtain more promising results.

Table 14. Top-1 accuracy of long-tailed recognition methods on the uniform test distribution.

Object	ImageNet-LT				CIFAR100-LT(IR10)				CIFAR100-LT(IR50)			
	Many	Med.	Few	All	Many	Med.	Few	All	Many	Med.	Few	All
Softmax	68.1	41.5	14.0	48.0	66.0	42.7	-	59.1	66.8	37.4	15.5	45.6
Causal [30]	64.1	45.8	27.2	50.3	63.3	49.9	-	59.4	62.9	44.9	26.2	48.8
Balanced Softmax [19]	64.1	48.2	33.4	52.3	43.4	55.7	-	61.0	62.1	45.6	36.7	50.9
MiSLAS [50]	62.0	49.1	32.8	51.4	64.9	56.6	-	62.5	61.8	48.9	33.9	51.5
LADE [16]	64.4	47.7	34.3	52.3	63.8	56.0	-	61.6	60.2	46.2	35.6	50.1
RIDE [36]	68.0	52.9	35.1	56.3	65.7	53.3	-	61.8	66.6	46.2	30.3	51.7
TADE (ours)	66.5	57.0	43.5	58.8	65.8	58.8	-	63.6	61.5	50.2	45.0	53.9

Object	CIFAR100-LT(IR100)				Places-LT				iNaturalist 2018			
	Many	Med.	Few	All	Many	Med.	Few	All	Many	Med.	Few	All
Softmax	68.6	41.1	9.6	41.4	46.2	27.5	12.7	31.4	74.7	66.3	60.0	64.7
Causal [30]	64.1	46.8	19.9	45.0	23.8	35.7	39.8	32.2	71.0	66.7	59.7	64.4
Balanced Softmax [19]	59.5	45.4	30.7	46.1	42.6	39.8	32.7	39.4	70.9	70.7	70.4	70.6
MiSLAS [50]	60.4	49.6	26.6	46.8	41.6	39.3	27.5	37.6	71.7	71.5	69.7	70.7
LADE [16]	58.7	45.8	29.8	45.6	42.6	39.4	32.3	39.2	68.9	68.7	70.2	69.3
RIDE [36]	67.4	49.5	23.7	48.0	43.1	41.0	33.0	40.3	71.5	70.0	71.6	71.8
TADE (ours)	65.4	49.3	29.3	49.8	40.4	43.2	36.8	40.9	74.5	72.5	73.0	72.9

Table 15. Top-1 accuracy on CIFAR10-LT, where the test class distribution is uniform. Most results are directly copied from the work [50].

Imbalance Ratio	Softmax	BBN	MiSLAS	RIDE	TADE (ours)
10	86.4	88.4	90.0	89.7	90.8
100	70.4	79.9	82.1	81.6	83.8

D.3. More Results on Uniform Test Distribution

In the main paper, we provide overall performance on the uniform test class distribution. Here, we further report the accuracy in terms of three sets of classes. As shown in Table 14, our method achieves the state-of-the-art performance in terms of overall accuracy on all datasets. For example, compared with the current state-of-the-art RIDE method [36], TADE obtains 2.5 top-1 accuracy gain on ImageNet-LT and 1.1 performance gain on iNaturalist 2018.

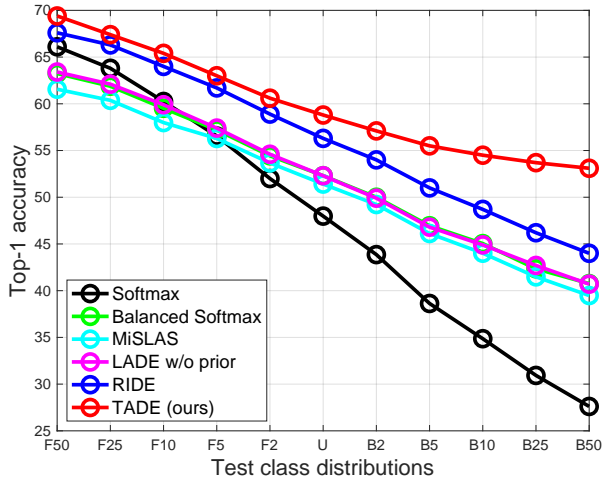
Note that Softmax obtains the best performance on many-shot classes, since it directly simulates the original training long-tailed distributions, thus being skilled in head classes. However, it performs quite poorly on medium-shot and few-shot classes. In contrast, our method can obtain a better trade-off between different groups of classes, thus achieving better overall performance.

In addition, we also conduct experiments on CIFAR10-LT with imbalance ratios 10 and 100. The promising results in Table 15 further demonstrate the effectiveness of our proposed method.

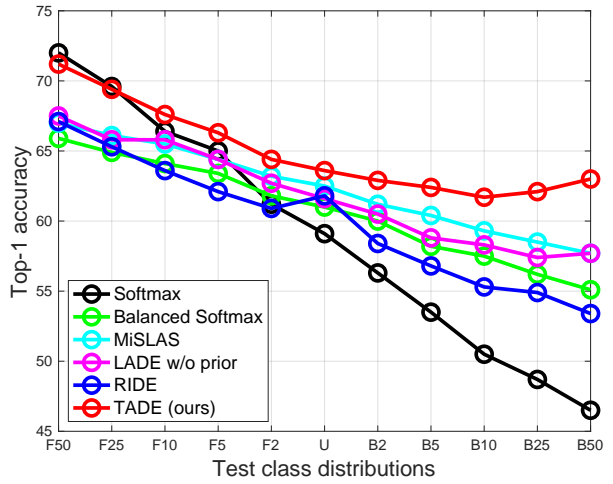
D.4. More Results on Diverse Test Distributions

In the main paper, we provide the overall performance on diverse unknown test class distributions in terms of top-1 accuracy. In this appendix, we further report the accuracy in terms of three sets of classes for each test class distribution on all datasets. As shown in Table 13, by using the test-time self-supervised aggregation strategy, our method is able to obtain better performance on the dominant test classes, thus achieving better performance on the diverse test class distributions.

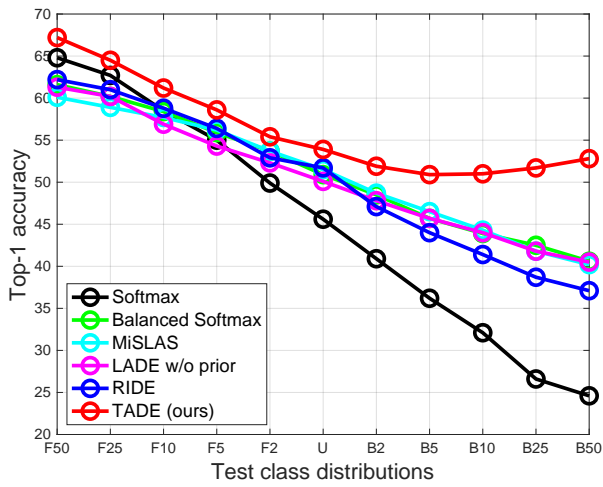
We also plot the results on different test class distributions in Figure 4. To be specific, Softmax only performs well on the highly-imbalanced forward long-tailed class distributions. Existing state-of-the-art long-tailed recognition baselines show better performance than Softmax, but they cannot handle the backward test class distributions well. In contrast, our method consistently outperforms compared methods on all benchmark datasets. Note that on the backward long-tailed test distributions with a relatively large imbalance ratio, the performance improvement is more significant.



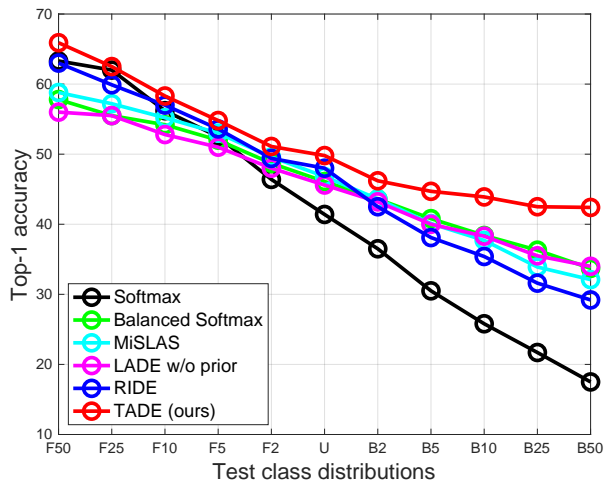
(a) ImageNet-LT



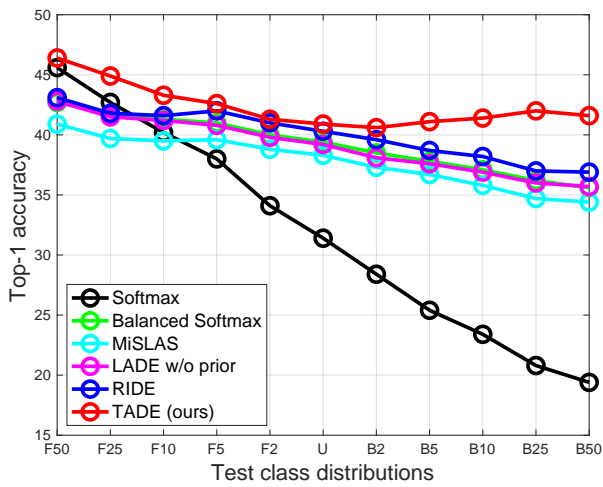
(b) CIFAR100-LT(IR10)



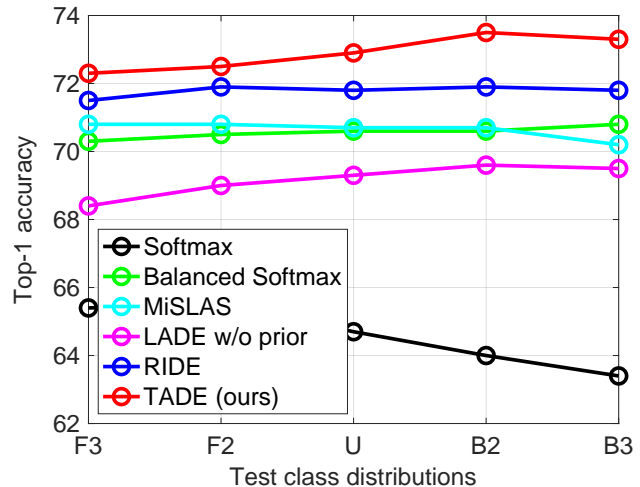
(c) CIFAR100-LT(IR50)



(d) CIFAR100-LT(IR100)



(e) Places-LT



(f) iNaturalist 2018

Figure 4. Performance visualizations on diverse unknown test class distributions, where “F” indicates the forward long-tailed distributions as training data, “B” indicates the backward long-tailed distributions to the training data, and “U” denotes the uniform distribution.

E. Ablation Studies on Expert Learning

E.1. Discussion on Expert Number

Our approach can be straightforwardly extended to more than three experts. For the models with more experts, we can adjust the parameters in the expertise-guided loss functions so that different experts are skilled in different types of class distributions. Following this, we further test the influence of the expert number on our method. As shown in Table 16, with the increasing number of experts, the ensemble performance of our method is improved, *e.g.*, four experts can obtain 1.2 performance gain than three experts.

In TADE, we consider three experts because the “forward” and “backward” experts are necessary since they span a wide spectrum of possible test class distributions, while the “uniform” expert ensures that we retain high accuracy on the uniform test class distributions. Note that three experts are sufficient to provide a good trade-off between performance and efficiency.

Table 16. Performance of our method with different expert numbers on ImageNet-LT with the uniform test distribution.

Object	3 experts			
	Many-shot	Medium-shot	Few-shot	All classes
Expert E_1	68.8	43.7	17.2	49.8
Expert E_2	65.5	50.5	33.3	53.9
Expert E_3	43.4	48.6	53.9	47.3
Ensemble	67.0	56.7	42.6	58.8
Object	4 experts			
	Many-shot	Medium-shot	Few-shot	All classes
Expert E_1	69.4	44.5	16.5	50.3
Expert E_2	66.2	51.5	32.9	54.6
Expert E_3	55.7	52.7	46.8	53.4
Expert E_4	44.1	49.7	55.9	48.4
Ensemble	66.6	58.4	46.7	60.0
Object	5 experts			
	Many-shot	Medium-shot	Few-shot	All classes
Expert E_1	69.8	44.9	17.0	50.7
Expert E_2	68.8	48.4	23.9	52.9
Expert E_3	66.1	51.4	22.0	54.5
Expert E_4	56.8	52.7	47.7	53.6
Expert E_5	43.1	59.0	54.8	47.5
Ensemble	68.8	58.5	43.2	60.4
Object	6 experts			
	Many-shot	Medium-shot	Few-shot	All classes
Expert E_1	69.0	35.1	6.51	44.3
Expert E_2	69.6	44.3	16.6	50.3
Expert E_3	66.0	51.2	32.2	54.3
Expert E_4	56.1	52.5	47.4	53.2
Expert E_5	43.2	49.2	55.5	47.8
Expert E_6	31.6	43.8	58.3	41.0
Ensemble	66.9	59.4	46.5	60.5

E.2. Hyper-Parameters in Inverse Softmax Loss

This appendix evaluates the influence of the hyper-parameter λ in the inverse softmax loss for the backward expert, where we fix the losses for the forward and the uniform experts, and only adjust the value of λ . As shown in Table 17, with the increase of λ , the backward expert simulates more inversely long-tailed distribution (to the training data), and thus the ensemble performance on few-shot classes is better. Considering the performance trade-off between head classes and tail classes, when $\lambda \in \{2, 3\}$, our method achieves relatively better performance on ImageNet-LT.

Table 17. Influence of the hyper-parameter λ in the proposed inverse softmax loss on ImageNet-LT with the uniform test distribution.

Object	$\lambda = 0.5$			
	Many-shot	Medium-shot	Few-shot	All classes
Expert E_1	69.1	43.6	17.2	49.8
Expert E_2	66.4	50.9	33.4	54.5
Expert E_3	61.9	51.9	40.3	54.2
Ensemble	71.0	54.6	33.4	58.0
Object	$\lambda = 1$			
	Many-shot	Medium-shot	Few-shot	All classes
Expert E_1	69.7	44.0	16.8	50.2
Expert E_2	65.5	51.1	32.4	54.4
Expert E_3	56.5	52.3	47.1	53.2
Ensemble	77.2	55.7	36.2	58.6
Object	$\lambda = 2$			
	Many-shot	Medium-shot	Few-shot	All classes
Expert E_1	68.8	43.7	17.2	49.8
Expert E_2	65.5	50.5	33.3	53.9
Expert E_3	43.4	48.6	53.9	47.3
Ensemble	67.0	56.7	42.6	58.8
Object	$\lambda = 3$			
	Many-shot	Medium-shot	Few-shot	All classes
Expert E_1	69.6	43.8	17.4	50.2
Expert E_2	66.2	50.7	33.1	54.2
Expert E_3	43.4	48.6	53.9	48.0
Ensemble	67.8	56.8	42.4	59.1
Object	$\lambda = 4$			
	Many-shot	Medium-shot	Few-shot	All classes
Expert E_1	69.1	44.1	16.3	49.9
Expert E_2	65.7	50.8	32.6	54.1
Expert E_3	21.9	38.1	58.9	34.7
Ensemble	60.2	57.5	50.4	57.6
Object	$\lambda = 5$			
	Many-shot	Medium-shot	Few-shot	All classes
Expert E_1	69.7	43.7	16.5	50.0
Expert E_2	65.9	50.9	33.0	54.2
Expert E_3	16.0	33.9	60.6	30.6
Ensemble	56.3	57.5	54.0	56.6

Table 18. The influence of the epoch number on the learned expert weights by test-time self-supervised learning on ImageNet-LT.

Test Dist.	Epoch 1			Epoch 5			Epoch 10		
	E1 (w_1)	E2 (w_2)	E3 (w_3)	E1 (w_1)	E2 (w_2)	E3 (w_3)	E1 (w_1)	E2 (w_2)	E3 (w_3)
Forward-50	0.44	0.33	0.23	0.52	0.35	0.13	0.52	0.37	0.11
Forward-25	0.43	0.34	0.23	0.50	0.35	0.15	0.50	0.37	0.13
Forward-10	0.43	0.34	0.23	0.46	0.36	0.18	0.46	0.36	0.18
Forward-5	0.41	0.34	0.25	0.43	0.34	0.23	0.43	0.35	0.22
Forward-2	0.37	0.33	0.30	0.37	0.35	0.28	0.38	0.33	0.29
Uniform	0.34	0.31	0.35	0.33	0.33	0.34	0.33	0.32	0.35
Backward-2	0.30	0.32	0.38	0.29	0.31	0.40	0.29	0.32	0.39
Backward-5	0.27	0.29	0.44	0.24	0.31	0.45	0.23	0.31	0.46
Backward-10	0.24	0.29	0.47	0.21	0.29	0.50	0.21	0.30	0.49
Backward-25	0.23	0.29	0.48	0.18	0.29	0.53	0.17	0.3	0.53
Backward-50	0.24	0.29	0.47	0.17	0.27	0.56	0.15	0.28	0.57

Test Dist.	Epoch 20			Epoch 50			Epoch 100		
	E1 (w_1)	E2 (w_2)	E3 (w_3)	E1 (w_1)	E2 (w_2)	E3 (w_3)	E1 (w_1)	E2 (w_2)	E3 (w_3)
Forward-50	0.53	0.38	0.09	0.53	0.38	0.09	0.53	0.38	0.09
Forward-25	0.51	0.37	0.12	0.52	0.37	0.11	0.50	0.38	0.12
Forward-10	0.44	0.36	0.20	0.45	0.37	0.18	0.46	0.36	0.18
Forward-5	0.42	0.35	0.23	0.42	0.35	0.23	0.42	0.35	0.23
Forward-2	0.38	0.33	0.29	0.39	0.33	0.28	0.38	0.32	0.30
Uniform	0.33	0.33	0.34	0.34	0.32	0.34	0.32	0.33	0.35
Backward-2	0.29	0.31	0.40	0.30	0.32	0.38	0.29	0.30	0.41
Backward-5	0.24	0.31	0.45	0.23	0.29	0.48	0.25	0.30	0.45
Backward-10	0.20	0.30	0.50	0.21	0.31	0.48	0.21	0.30	0.49
Backward-25	0.16	0.30	0.54	0.17	0.29	0.54	0.17	0.30	0.53
Backward-50	0.15	0.29	0.56	0.14	0.29	0.57	0.14	0.29	0.57

Table 19. The influence of the batch size on the learned expert weights by test-time self-supervised learning on ImageNet-LT.

Test Dist.	Batch size 64			Batch size 128			Batch size 256		
	E1 (w_1)	E2 (w_2)	E3 (w_3)	E1 (w_1)	E2 (w_2)	E3 (w_3)	E1 (w_1)	E2 (w_2)	E3 (w_3)
Forward-50	0.52	0.37	0.11	0.52	0.35	0.13	0.50	0.33	0.17
Forward-25	0.49	0.38	0.13	0.50	0.35	0.15	0.48	0.24	0.18
Forward-10	0.46	0.36	0.18	0.46	0.36	0.18	0.45	0.35	0.20
Forward-5	0.44	0.34	0.22	0.43	0.34	0.23	0.43	0.35	0.22
Forward-2	0.37	0.34	0.29	0.37	0.35	0.28	0.38	0.33	0.29
Uniform	0.34	0.32	0.34	0.33	0.33	0.34	0.33	0.32	0.35
Backward-2	0.28	0.32	0.40	0.29	0.31	0.40	0.30	0.31	0.39
Backward-5	0.24	0.30	0.46	0.24	0.31	0.45	0.25	0.30	0.45
Backward-10	0.21	0.30	0.49	0.21	0.29	0.50	0.22	0.29	0.49
Backward-25	0.17	0.29	0.54	0.18	0.29	0.53	0.20	0.28	0.52
Backward-50	0.15	0.30	0.55	0.17	0.27	0.56	0.19	0.27	0.54

F. Ablation Studies on Test-time Learning

F.1. Influences of Training Epoch

In previous results, we set the training epoch of test-time self-supervised learning to 5 on all datasets. Here, we further evaluate the influence of the epoch number, where we adjust the epoch number from 1 to 100. As shown in Table 18, when the training epoch number is larger than 5, the learned expert weights by our method are converged, which verifies that our method is robust enough and does not have degenerate solutions on ImageNet-LT. The corresponding performance on diverse test distributions is reported in Table 20.

F.2. Influences of Batch Size

In previous results, we set the batch size of the test-time self-supervised learning strategy to 128 on all datasets. In this appendix, we further evaluate the influence of the batch size on our strategy, where we adjust the batch size from 64 to 256. As shown in Table 19, with different batch sizes, the learned expert weights by our method keep nearly the same, which shows that our method is insensitive to the batch size. The corresponding performance on diverse test class distributions is reported in Table 21, where the performance is also nearly the same when using different batch sizes.

Table 20. The influence of the epoch number on the performance of test-time self-supervised learning on ImageNetL-LT.

Test Dist.	Epoch 1				Epoch 5				Epoch 10			
	Many	Med.	Few	All	Many	Med.	Few	All	Many	Med.	Few	All
Forward-50	68.8	54.6	37.5	68.5	70.0	53.2	33.1	69.4	70.1	52.9	32.4	69.5
Forward-25	68.6	54.9	34.9	66.9	69.5	53.2	32.2	67.4	69.7	52.5	32.5	67.5
Forward-10	60.3	55.3	37.6	65.2	69.9	54.3	34.7	65.4	69.9	54.5	35.0	65.4
Forward-5	68.4	55.3	37.3	63.0	68.9	54.8	35.8	63.0	68.8	54.9	36.0	63.0
Forward-2	67.9	56.2	40.8	60.6	68.2	56.0	40.1	60.6	68.2	56.0	39.7	60.5
Uniform	66.7	56.9	43.1	58.8	66.5	57.0	43.5	58.8	66.4	56.9	43.4	58.8
Backward-2	65.6	57.1	44.7	57.1	65.3	57.1	45.0	57.1	65.3	57.1	45.0	57.1
Backward-5	63.9	57.6	46.8	55.5	63.4	56.4	47.5	55.5	63.3	57.4	47.8	55.6
Backward-10	62.1	57.6	47.9	54.2	60.9	57.5	50.1	54.5	61.1	57.6	48.9	54.5
Backward-25	62.4	57.6	48.5	53.4	60.5	57.1	50.0	53.7	60.5	57.1	50.3	53.8
Backward-50	64.9	56.7	47.8	51.9	60.7	56.2	50.7	53.1	60.1	55.9	51.2	53.2

Test Dist.	Epoch 20				Epoch 50				Epoch 100			
	Many	Med.	Few	All	Many	Med.	Few	All	Many	Med.	Few	All
Forward-50	70.3	52.2	32.4	69.5	70.3	52.2	32.4	69.5	70.0	52.2	32.4	69.3
Forward-25	69.8	52.4	31.4	67.5	69.9	52.3	31.4	67.6	69.7	52.6	32.6	67.5
Forward-10	69.6	54.8	35.8	65.3	69.8	54.6	35.2	65.4	69.8	54.6	35.0	65.4
Forward-5	68.7	55.0	36.4	63.0	68.	55.0	36.4	63.0	68.7	54.7	36.7	62.9
Forward-2	68.1	56.0	39.9	60.5	68.3	55.9	39.6	60.5	68.2	56.0	40.1	60.6
Uniform	66.7	56.9	43.2	58.8	66.9	56.8	42.8	58.8	66.5	56.8	43.2	58.7
Backward-2	65.4	57.1	44.9	57.1	65.6	57.0	44.7	57.1	64.9	57.0	45.6	57.0
Backward-5	63.4	57.4	47.6	55.5	62.7	57.4	48.3	55.6	63.4	57.5	47.0	55.4
Backward-10	60.7	57.5	49.4	54.6	61.1	57.6	48.8	54.4	60.6	57.6	49.1	54.5
Backward-25	60.4	57.1	50.4	53.9	60.4	57.0	50.3	53.8	60.9	56.8	50.2	53.7
Backward-50	60.9	56.1	51.1	53.2	60.6	55.9	51.1	53.2	60.8	56.1	51.2	53.2

Table 21. The influence of the batch size on the performance of test-time self-supervised learning on ImageNetL-LT.

Test Dist.	Batch size 64				Batch size 128				Batch size 256			
	Many	Med.	Few	All	Many	Med.	Few	All	Many	Med.	Few	All
Forward-50	70.0	52.6	33.8	69.3	70.0	53.2	33.1	69.4	69.7	53.8	34.6	69.2
Forward-25	69.6	53.0	33.3	67.5	69.5	53.2	32.2	67.4	69.2	53.7	32.8	67.2
Forward-10	69.9	54.3	34.8	65.4	69.9	54.3	34.7	65.4	69.5	55.0	35.9	65.3
Forward-5	69.0	54.6	35.6	63.0	68.9	54.8	35.8	63.0	68.8	54.9	36.0	63.0
Forward-2	68.2	56.0	40.0	60.6	68.2	56.0	40.1	60.6	68.1	56.0	40.1	60.5
Uniform	66.9	56.6	42.4	58.8	66.5	57.0	43.5	58.8	66.5	56.9	43.3	58.8
Backward-2	64.9	57.0	45.7	57.0	65.3	57.1	45.0	57.1	65.5	57.1	44.8	57.1
Backward-5	63.1	57.4	47.3	55.4	63.4	56.4	47.5	55.5	63.4	56.4	47.5	55.5
Backward-10	60.9	57.7	48.6	54.4	60.9	57.5	50.1	54.5	61.3	57.6	48.7	54.4
Backward-25	60.8	56.7	50.1	53.6	60.5	57.1	50.0	53.7	61.0	57.2	49.6	53.6
Backward-50	61.1	56.2	50.8	53.1	60.7	56.2	50.7	53.1	61.2	56.4	50.0	52.9

Table 22. The influence of the learning rate on the learned expert weights by test-time self-supervised learning on ImageNetL-LT, where the number of the training epoch is 5.

Test Dist.	Learning rate 0.001			Learning rate 0.01			Learning rate 0.025		
	E1 (w_1)	E2 (w_2)	E3 (w_3)	E1 (w_1)	E2 (w_2)	E3 (w_3)	E1 (w_1)	E2 (w_2)	E3 (w_3)
Forward-50	0.36	0.34	0.30	0.49	0.33	0.18	0.52	0.35	0.13
Forward-25	0.36	0.34	0.30	0.48	0.34	0.18	0.50	0.35	0.15
Forward-10	0.36	0.34	0.30	0.45	0.34	0.21	0.46	0.36	0.18
Forward-5	0.36	0.33	0.31	0.43	0.34	0.23	0.43	0.34	0.23
Forward-2	0.35	0.33	0.32	0.38	0.33	0.29	0.37	0.35	0.28
Uniform	0.33	0.33	0.34	0.34	0.33	0.33	0.33	0.33	0.34
Backward-2	0.32	0.32	0.36	0.30	0.32	0.38	0.29	0.31	0.40
Backward-5	0.31	0.32	0.37	0.25	0.31	0.44	0.24	0.31	0.45
Backward-10	0.31	0.32	0.37	0.22	0.29	0.49	0.21	0.29	0.50
Backward-25	0.31	0.32	0.37	0.21	0.28	0.51	0.18	0.29	0.53
Backward-50	0.31	0.32	0.37	0.20	0.28	0.52	0.17	0.27	0.56

Test Dist.	Learning rate 0.05			Learning rate 0.1			Learning rate 0.5		
	E1 (w_1)	E2 (w_2)	E3 (w_3)	E1 (w_1)	E2 (w_2)	E3 (w_3)	E1 (w_1)	E2 (w_2)	E3 (w_3)
Forward-50	0.53	0.36	0.11	0.53	0.37	0.10	0.57	0.34	0.09
Forward-25	0.51	0.36	0.13	0.52	0.36	0.12	0.57	0.34	0.09
Forward-10	0.45	0.37	0.18	0.47	0.36	0.18	0.44	0.36	0.20
Forward-5	0.42	0.35	0.23	0.47	0.36	0.18	0.39	0.36	0.25
Forward-2	0.38	0.24	0.28	0.42	0.36	0.22	0.36	0.34	0.30
Uniform	0.33	0.33	0.34	0.31	0.31	0.38	0.33	0.34	0.33
Backward-2	0.30	0.31	0.39	0.31	0.30	0.39	0.29	0.31	0.40
Backward-5	0.24	0.31	0.45	0.24	0.29	0.47	0.21	0.28	0.51
Backward-10	0.21	0.30	0.49	0.21	0.31	0.48	0.22	0.32	0.46
Backward-25	0.16	0.28	0.56	0.17	0.31	0.52	0.15	0.30	0.55
Backward-50	0.15	0.28	0.57	0.14	0.28	0.58	0.12	0.27	0.61

F.3. Influences of Learning Rate

In this appendix, we evaluate the influence of the learning rate on our strategy, where we adjust the learning rate from 0.001 to 0.5. As shown in Table 22, with the increase of the learning rate, the learned expert weights by our method are sharper and fit the unknown test class distributions better. For example, when the learning rate is 0.001, the weight for expert E_1 is 0.36 on the forward-50 test distribution, while when the learning rate increases to 0.5, the weight for expert E_1 becomes 0.57 on the forward-50 test distribution. Similar phenomena can also be observed on backward long-tailed test class distributions.

By observing the corresponding model performance on diverse test class distributions in Table 23, we find that when the learning rate is too small (e.g., 0.001), our test-time self-supervised aggregation strategy is unable to converge, given a fixed training epoch number 5. In contrast, given the same training epochs, our method can obtain better performance by reasonably increasing the learning rate. Note that, a too-large learning rate may also degenerate the model.

F.4. Results of Prediction Confidence

In our theoretical analysis, we find that our test-time self-supervised aggregation strategy not only simulates the test class distribution, but also makes the model prediction more confident. In this appendix, we further evaluate whether our strategy indeed improves the prediction confidence of models on diverse unknown test class distributions of ImageNet-LT. Therefore, we compare the prediction confidence of our method without and with test-time self-supervised aggregation in terms of the hard mean of the highest prediction probability on all test samples.

As shown in Table 24, our test-time self-supervised aggregation strategy enables the deep model to have higher prediction confidence. For example, on the forward-50 test distribution, our strategy obtains 0.015 confidence improvement, which is non-trivial since it is an average value for a large number of samples (more than 10,000 samples). In addition, when the class imbalance ratio becomes larger, our method is able to obtain more significant confidence improvement.

Table 23. The influence of the learning rate on the performance of test-time self-supervised learning on ImageNet-LT, where the number of the training epoch is 5.

Test Dist.	Learning rate 0.001				Learning rate 0.01				Learning rate 0.025			
	Many	Med.	Few	All	Many	Med.	Few	All	Many	Med.	Few	All
Forward-50	67.3	56.1	44.1	67.3	69.5	54.0	34.6	69.0	70.0	53.2	33.1	69.4
Forward-25	67.4	56.2	40.3	66.1	69.2	53.8	33.2	67.2	69.5	53.2	32.2	67.4
Forward-10	67.7	56.4	41.9	64.5	69.6	55.0	36.1	65.4	69.9	54.3	34.7	65.4
Forward-5	67.2	55.9	40.8	62.6	68.7	55.0	36.2	63.0	68.9	54.8	35.8	63.0
Forward-2	67.5	56.2	41.7	60.5	68.1	56.0	40.1	60.5	68.2	56.0	40.1	60.6
Uniform	66.9	56.6	42.7	58.8	67.0	56.8	42.7	58.8	66.5	57.0	43.5	58.8
Backward-2	66.5	56.8	43.3	56.9	65.5	57.1	44.8	57.1	65.3	57.1	45.0	57.1
Backward-5	65.8	57.5	43.7	55.0	63.9	57.5	46.9	55.5	63.4	56.4	47.5	55.5
Backward-10	64.6	57.5	43.7	53.1	61.3	57.6	48.6	54.4	60.9	57.5	50.1	54.5
Backward-25	66.0	57.3	44.1	51.5	61.1	57.4	49.3	53.5	60.5	57.1	50.0	53.7
Backward-50	68.2	56.8	43.7	50.0	63.1	56.5	49.5	52.7	60.7	56.2	50.7	53.1

Test Dist.	Learning rate 0.05				Learning rate 0.1				Learning rate 0.5			
	Many	Med.	Few	All	Many	Med.	Few	All	Many	Med.	Few	All
Forward-50	70.2	52.4	32.4	69.5	70.3	52.3	32.4	69.5	70.3	51.2	32.4	69.5
Forward-25	69.7	52.5	32.5	67.5	69.9	52.3	31.4	67.6	69.9	51.1	29.5	67.5
Forward-10	69.7	54.7	35.8	65.4	69.9	54.3	34.8	65.4	69.5	55.0	35.8	65.3
Forward-5	68.8	54.9	36.2	63.0	68.8	54.8	36.1	63.0	68.3	55.3	37.6	62.9
Forward-2	68.3	56.0	39.6	60.5	68.0	56.1	40.2	60.5	67.1	56.5	42.3	60.5
Uniform	66.6	56.9	43.2	58.8	65.6	57.1	44.7	58.7	67.8	56.4	40.9	58.7
Backward-2	65.4	57.1	44.9	57.1	65.6	57.0	44.5	57.0	65.3	57.1	45.2	57.1
Backward-5	63.6	57.5	48.9	55.4	63.0	57.4	48.1	55.6	61.4	57.4	49.2	55.6
Backward-10	61.1	57.5	48.9	54.4	61.3	57.6	48.6	54.4	62.0	57.5	47.9	54.2
Backward-25	59.9	56.8	51.0	53.9	60.9	57.2	49.9	53.7	60.2	56.8	50.8	53.9
Backward-50	60.1	56.0	51.2	53.2	59.6	55.8	51.3	53.2	58.2	55.6	52.2	53.5

Table 24. Comparison of prediction confidence between our method without and with test-time self-supervised aggregation on ImageNet-LT, in terms of the hard mean of the highest prediction probability on each sample. The higher of the highest prediction, the better of the model.

Method	Prediction confidence on ImageNet-LT											
	Forward					Uniform		Backward				
	50	25	10	5	2	1	2	5	10	25	50	
Ours w/o test-time learning	0.694	0.687	0.678	0.665	0.651	0.639	0.627	0.608	0.596	0.583	0.574	
Ours w test-time learning	0.711	0.704	0.689	0.674	0.654	0.639	0.625	0.609	0.599	0.589	0.583	

Table 25. Model complexity and performance of different methods in terms of the parameter number, Multiply–Accumulate Operations (MACs) and top-1 accuracy on test-agnostic long-tailed recognition. Here, we do not use the efficient expert assignment trick in [36] for RIDE and our method.

			ImageNet-LT (ResNeXt-50)										
Method	Params (M)	MACs (G)	Forward					Uniform	Backward				
			50	25	10	5	2	1	2	5	10	25	50
Softmax	25.03 (1.0x)	4.26 (1.0x)	66.1	63.8	60.3	56.6	52.0	48.0	43.9	38.6	34.9	30.9	27.6
RIDE [36]	38.28 (1.5x)	6.08 (1.4x)	67.6	66.3	64.0	61.7	58.9	56.3	54.0	51.0	48.7	46.2	44.0
TADE (ours)	38.28 (1.5x)	6.08 (1.4x)	69.4	67.4	65.4	63.0	60.6	58.8	57.1	55.5	54.5	53.7	53.1
			CIFAR100-LT-IR100 (ResNet-32)										
Method	Params (M)	MACs (G)	Forward					Uniform	Backward				
			50	25	10	5	2	1	2	5	10	25	50
Softmax	0.46 (1.0x)	0.07 (1.0x)	63.3	62.0	56.2	52.5	46.4	41.4	36.5	30.5	25.8	21.7	17.5
RIDE [36]	0.77 (1.5x)	0.10 (1.4x)	63.0	59.9	57.0	53.6	49.4	48.0	42.5	38.1	35.4	31.6	29.2
TADE (ours)	0.77 (1.5x)	0.10 (1.4x)	65.9	62.5	58.3	54.8	51.1	49.8	46.2	44.7	43.9	42.5	42.4
			Places-LT (ResNet-152)										
Method	Params (M)	MACs (G)	Forward					Uniform	Backward				
			50	25	10	5	2	1	2	5	10	25	50
Softmax	60.19 (1.0x)	11.56 (1.0x)	45.6	42.7	40.2	38.0	34.1	31.4	28.4	25.4	23.4	20.8	19.4
RIDE [36]	88.07 (1.5x)	13.18 (1.1x)	43.1	41.8	41.6	42.0	41.0	40.3	39.6	38.7	38.2	37.0	36.9
TADE (ours)	88.07 (1.5x)	13.18 (1.1x)	46.4	44.9	43.3	42.6	41.3	40.9	40.6	41.1	41.4	42.0	41.6
			iNaturalist 2018 (ResNet-50)										
Method	Params (M)	MACs (G)	Forward		Uniform	Backward							
			3	2	1	2	3						
Softmax	25.56 (1.0x)	4.14 (1.0x)	65.4	65.5	64.7	64.0	63.4						
RIDE [36]	39.07 (1.5x)	5.80 (1.4x)	71.5	71.9	71.8	71.9	71.8						
TADE (ours)	39.07 (1.5x)	5.80 (1.4x)	72.3	72.5	72.9	73.5	73.3						

G. More Discussions on Model Complexity

In this appendix, we discuss the model complexity of our method in terms of the number of parameters, multiply-accumulate operations (MACs) and top-1 accuracy on test-agnostic long-tailed recognition.

As shown in Table 25, both TADE and RIDE belong to ensemble learning based methods, so they have more parameters (about 1.5x) and MACs (about 1.4x) than the original backbone model, where we do not use the efficient expert assignment trick in [36] for both methods. Because of the ensemble effectiveness of the multi-expert scheme, both methods perform much better than non-ensemble methods (*e.g.*, Softmax and other long-tailed methods). In addition, since our method and RIDE use the same multi-expert framework, both methods have the same number of parameters and MACs. Nevertheless, by using our proposed skill-diverse expert learning and test-time self-supervised aggregation strategies, our method performs much better than RIDE with no increase in model parameters and computational costs.

One may concern that the multi-expert scheme leads to more model parameters and higher computational costs. However, note that the main focus of this paper is to solve the test-agnostic long-tailed recognition problem, while extensive promising results have shown that our method addresses this problem well. In this sense, slightly increasing the model complexity is acceptable in order to solve this practical and challenging problem. Moreover, since there have already been many studies [13, 37] showing effectiveness in improving the efficiency of the multi-expert scheme, we think the computation increment is not a very severe issue and we leave it for future work.